Origin of springtime ozone enhancements in the lower troposphere over Beijing: In situ measurements and model analysis

J. Huang[1,*], H. Liu[1], J. H. Crawford[2], C. Chan[3], D. B. Considine[3, 4], Y. Zhang[5], X. Zheng[6], C. Zhao[7], V. Thouret[8], S. J. Oltmans[9, 10], S. C. Liu[11], D. B. A. Jones[12], S. D. Steenrod[13, 14], and M. R. Damon[14, 15]

[1] National Institute of Aerospace, Hampton, VA, United States

[2] NASA Langley Research Center, Hampton, VA, United States

[3] Institute of Earth Environment, Chinese Academy of Sciences, Xi'an, China

[4] NASA Headquarters, Washington, D.C., United States

[5] South China Institute of Environmental Science, Guangzhou, Guangdong, China

[6] Chinese Academy of Meteorological Sciences, Beijing, China

[7] Peking University, Beijing, China

[8] Laboratoire d'Aérologie, UMR5560, Toulouse, France

[9] CIRES, University of Colorado, Boulder, CO, United States

[10] NOAA ESRL, Boulder, CO, United States

[11] Academia Sinica, Taipei, Taiwan

[12] University of Toronto, Toronto, Ontario, Canada

[13] Universities Space Research Association, Columbia, MD, United States

[14] NASA Goddard Space Flight Center, Greenbelt, MD, United States

[15] Science Systems and Applications Inc., Lanham, MD, United States

[*] now at: University of Washington, Seattle, WA, United States

Atmospheric Chemistry and Physics, revised, March 2015

Correspondence to: H. Liu (Hongyu.Liu-1@nasa.gov)

Abstract. Ozone (O_3) concentrations in the lower troposphere (LT) over Beijing have significantly increased over the past two decades as a result of rapid industrialization in China, with important implications for regional air quality and photochemistry of the background troposphere. We characterize the vertical distribution of lower-tropospheric (0-6km) O_3 over Beijing using observations from 16 ozonesonde soundings made during a field campaign in April-May 2005 and MOZAIC (Measurement of Ozone and Water Vapor by Airbus In-Service Aircraft) aircraft measurements over 13 days in the same period. We focus on the origin of LT O_3 enhancements observed over Beijing, particularly in May. We use a global 3-D chemistry and transport model (GEOS-Chem CTM) driven by assimilated meteorological fields to examine the transport pathways for O_3 pollution, and quantify the sources contributing to O_3 and its enhancements in the springtime LT over Beijing. Output from the Global Modeling Initiative (GMI) CTM is also used. High O_3 concentrations (up to 94.7 ppbv) were frequently observed at the altitude of ~1.5-2km. The CTMs captured the timing of the occurrences but significantly underestimated their magnitude. GEOS-Chem simulations and a case study showed that O_3 produced in the Asian troposphere (especially from Asian anthropogenic pollution) made major contributions to the observed O_3 enhancements. Contributions from anthropogenic pollution in the European and North American troposphere were reduced during these events, in contrast with days without O_3 enhancements, when contributions from Europe and North America were substantial. The O_3 enhancements typically occurred under southerly wind and warmer conditions. It is suggested that an earlier onset of the Asian summer monsoon would cause more O_3 enhancement events in the lower troposphere over the North China Plain in late spring and early summer.

1 Introduction

Tropospheric ozone (O_3) is an effective greenhouse gas, especially in the upper troposphere (UT) (Lacis et al., 1990). It is also the primary source of hydroxyl radicals (OH) that determine the oxidizing capacity of the atmosphere (Thompson, 1992). As an air pollutant near the surface, it has a detrimental effect on both vegetation and human health. Tropospheric O_3 has two sources - photochemical oxidation of hydrocarbons and carbon monoxide (CO) by OH radicals in the presence of oxides of nitrogen ($NO_x = NO + NO_2$), and downward transport from the stratosphere. Its precursors (NO_x, hydrocarbons, CO) are generated by fossil fuel combustion, industrial processes, biomass burning, vegetation, microbial activity in soils, and lightning.

Ozone concentrations have significantly increased in the lower troposphere (LT) across China (Chan et al., 2003; Ding et al., 2008; Wang et al., 2009) over the past decades as a result of increasing anthropogenic precursor emissions (Richter et al., 2005). Elevated O_3 levels not only lead to degradation of local and regional air quality (Wang et al., 2006; Wang et al. 2008; Lin et al., 2008), but also have significant implications for chemical environment and air quality in downwind regions (e.g., Hudman et al., 2004; Lin et al., 2012, 2014). Via deep convection or strong warm conveyor belts, Asian pollutants can be lifted up into the upper troposphere and transported to the North Pacific and North America (Jaffe et al., 1999; Liu et al., 2002, 2003; Liang et al., 2004; Cooper et al., 2010). This transpacific transport is most efficient in spring when cold fronts frequently occur and strong westerlies prevail in the upper troposphere over East Asia (Liu et al., 2003; Liang et al., 2004). Note, however, that stratospheric intrusions also maximize at mid-latitudes in spring. Ozonesonde measurements in western North America between 40°N and 55°N in April-May 2006 showed that stratospheric influences can be comparable to impacts of Asian transport (Doughty et al., 2011; Moody et al., 2012). Studies of the sources and variability of LT O_3 over China have also emphasized the roles of biomass burning emissions (Liu et al., 1999; Fu et al., 2007; Lin et al., 2009), biogenic emissions (Fu et al., 2007), and the impact of the Asian monsoon

system (Liu et al., 2002; Lin et al., 2009).

Located in northern China and with a population of over 19 million, Beijing is one of the world's largest cities and facing a severe problem of O_3 pollution. Ozone measurements over Beijing, derived from MOZAIC (Measurement of Ozone and Water Vapor by Airbus In-Service Aircraft) aircraft data from 1995 to 2005, showed that O_3 in the LT has increased by 2% annually and ~4% during May-July in contrast to flat or negative trends of other mega-cities at a similar latitude (Tokyo, New York, and Paris), and also exhibited higher daytime O_3 concentrations than these cities (Ding et al., 2008). Wang et al. (2012) reported a summertime increase rate of 3.4%yr^{-1} in the lower-tropospheric (0-3km) partial O_3 column over Beijing based on ozonesonde measurements from 2002 to 2012. In addition to the long-term positive trend, O_3 over Beijing often experiences high-concentration episodes at ground level. Wang et al. (2006) reported that in 13 out of 39 days of surface observations at an elevated site (280 meters asl) in northern Beijing during June-July 2005, ambient O_3 levels exceeded 120 ppbv and had a 1-hr maximum level of 286 ppbv. The IASI (Infrared Atmospheric Sounding Interferometer) observed O_3 concentrations in the LT (3km) over Beijing up to 10 ppbv higher than the values for the 40-50°N latitude band climatology, which is more representative of background O_3 (Dufour et al., 2010). Dufour et al. reported that the lower-tropospheric partial (0-6km) column O_3 in Beijing shows a sharp increase in late spring with a maximum in May.

High ground-level O_3 in Beijing is caused not only by local anthropogenic emissions but also by regional and long-range transport. As reported by Streets et al. (2007), 35-60% of O_3 during high-O_3 episodes at Beijing Olympic Stadium originated from sources outside Beijing. Back-trajectory analysis by Ding et al. (2008) indicated that elevated O_3 levels in the boundary layer over Beijing during May-July were mostly related to emissions from the North China Plain. However, past investigations of the sources and transport of lower-tropospheric O_3 in Beijing have mostly involved categorizing wind directions or calculating back trajectories, techniques that do not allow its various sources to be quantified. In addition, previous studies were mainly based on surface measurements, which are not

adequate for a full understanding of processes that control the vertical distribution and variability of lower-tropospheric O_3 in Beijing.

To characterize the distribution and variability and quantify the sources of springtime lower-tropospheric O_3 in Beijing, we analyze O_3 vertical profiles measured during an ozonesonde sounding campaign, as well as aircraft measurements made by MOZAIC program. We show that O_3 enhancements in the LT over Beijing were frequently observed by ozonesondes during April-May 2005. Such O_3 enhancements during some of those days were also captured by the MOZAIC aircraft. We apply the GEOS-Chem chemistry and transport model (CTM), driven by assimilated winds, to quantify the sources contributing to these O_3 enhancements over Beijing and examine the corresponding pollution transport pathways in East China. By tagging O_3 originating in different source regions and conducting sensitivity simulations, we show that these O_3 enhancements were mainly due to Asian anthropogenic pollution, while the impact of the European and North American emissions were significantly smaller. We find that the high O_3 episodes occurred mostly under southerly wind conditions. We also evaluate the Global Modeling Initiative (GMI) CTM simulations with observations, and show that current global models significantly underestimated the magnitude of these O_3 enhancements.

This paper is structured as follows. The ozonesonde and aircraft measurements, as well as GEOS-Chem and GMI CTM are briefly described in Section 2. We describe the characteristics of the distribution and variability of springtime lower-tropospheric O_3 in Beijing from ozonesonde observations and MOZAIC aircraft measurements in Section 3. The model performance in reproducing the observed characteristics is examined in Section 4. The model analysis and case study of various sources of lower-tropospheric O_3 enhancements are presented in Section 5, followed by summary and conclusions in Section 6.

2 Data and methods

2.1 Ozonesonde and aircraft measurements

We use two sets of in-situ O_3 vertical profiles over Beijing obtained during April-May 2005: One from the Transport of Air Pollutants and Tropospheric Ozone over China (TAPTO-China) (Chan et al., 2007; Zhang et al., 2012) ozonesonde campaign, and the other from the MOZAIC aircraft program (Marenco et al., 1998). The concurrent availability of these two data sets provides an excellent opportunity for cross-validation.

TAPTO-China was an intensive ozonesonde sounding campaign over China, conducted at five locations across southern China in the spring of 2004 (Zhang et al., 2012) and four locations across northern China in the spring of 2005. The main objective of TAPTO-China was to investigate the mechanisms controlling the spatio-temporal distribution, variability, and sources of springtime tropospheric O_3 over China and its surrounding regions. Figure 1 shows the locations of the four ozonesonde stations in northern China during the second phase of TAPTO-China (April-May 2005): Xining (36.43^{o}N, 101.45^{o}E), Beijing (39.80^{o}N, 116.18^{o}E), Longfengshan (44.44^{o}N, 127.36^{o}E), and Aletai (47.73^{o}N, 88.08^{o}E). In this study, we use the ozonesonde sounding data obtained at the Beijing station (34 meters asl), which is located in the suburban Daxin district of southeastern Beijing. Sixteen ENSCI-ECC ozonesonde (with Vaisala RS 80 radiosonde) soundings in total were performed at this station during April 11 – May 15, 2005, with one sounding every 2-3 days on average. These sondes were launched at 13:30 local time, and the air was sampled every 15s. Pollution at the station is expected to be heavier than the average in the city because it is located downwind of Beijing. All raw ozonesonde data were averaged into 100m bins.

The MOZAIC program was initiated in 1993 to collect experimental data of O_3 and water vapor obtained by five long-range commercial airlines flying all over the world. Its goal was to provide a large database for studies of atmospheric chemical and physical processes in order to improve chemistry and transport models (Marenco et al., 1998). Dual-beam UV absorption analyzers (Model 49-103 from Thermo Environment Instruments) were installed onboard the aircraft to measure O_3, and were calibrated in the laboratory every 6-12 months with an overall precision of +/- (2ppb + 2%) (Thouret et al., 1998; Thouret et al., 2006). Tropospheric O_3 measurements were routinely conducted during the ascents and descents of

flights nearby 50 cities frequented by MOZAIC operation (Marenco et al., 1998), including Beijing. More information about the MOZAIC program can be found on its website (http://www.iagos.fr/web/rubrique36.htm). The Beijing Capital International Airport is located about 25 km southeast of the urban Beijing area, and is surrounded by the mountains to the west, north, and northeast (Ding et al., 2008). MOZAIC obtained vertical O_3 profiles in Beijing from March 1995 through March 2006. For April-May 2005, 13 profiles are available. The raw data were sampled every 4s (~30m) vertically and averaged into 150m bins.

2.2 CTM simulations

GEOS-Chem is a global 3-D model of tropospheric chemistry driven by assimilated meteorological observations from the Goddard Earth Observing System (GEOS) of the NASA Global Modeling and Assimilation Office (GMAO). The use of assimilated meteorological data to drive the model makes it an ideal tool for explaining the factors governing observed constituent distributions for a specific year. The description and evaluation of GEOS-Chem as applied to tropospheric O_3-NO_x-hydrocarbon chemistry was first presented by Bey et al. (2001b), and a description of the coupled oxidant-aerosol simulation was given by Park et al. (2004). The reader is referred to the Appendix for a brief description of other aspects of the model, including the emissions used. Here, we use GEOS-Chem version v9-01-02 (http://www.geos-chem.org) driven by two generations of GEOS assimilated meteorological fields, GEOS-4 (Bloom et al., 2005) and GEOS-5 (Rienecker et al., 2008) with a degraded horizontal resolution (2°×2.5°). The two sets of meteorological input data allow for examination of the sensitivity of model results to uncertainties in our characterization of the April/May 2005 meteorology. While GEOS-Chem is the major modeling analysis tool we use, we also use outputs from simulations made with GMI CTM (http://gmi.gsfc.nasa.gov) (e.g., Strahan et al., 2007; Duncan et al., 2007; Considine et al., 2008; Allen et al., 2010) to take into account the uncertainty in model simulations. GMI CTM combines both tropospheric and stratospheric chemical mechanisms. GMI simulations are driven by the GEOS-4 and MERRA (i.e., GEOS-5.2.0) meteorological

data sets (2°×2.5°).

We use GEOS-Chem to investigate the contributions to the LT O_3 in Beijing from six source regions: troposphere of Asia, Africa, Europe, North America, the stratosphere, and the rest of the world. Figure 2 shows the tropospheric O_3 source regions defined in the model for tagged O_3 simulations. Ozone produced in each of these source regions is transported separately in the model, and removed by chemical loss and dry deposition at the same frequencies as those for total O_3. The sum of all tagged O_3 tracers is equivalent to the O_3 concentration from the standard full-chemistry simulation (Wang et al., 1998). This approach was previously applied to a number of investigations (e.g., Liu et al., 2002; Liu et al., 2009; Zhang et al., 2012). However, it is important to note that tagged O_3 by source regions does not represent the sensitivity of tropospheric O_3 to emissions in those regions. This is because O_3 precursors themselves can be transported out of their source regions and can therefore contribute to O_3 production elsewhere.

We therefore also conduct sensitivity simulations to examine the effect of various emission types on tropospheric O_3 over Beijing. In these simulations, emissions from Asian fossil fuel, biomass burning, European fossil fuel, North American fossil fuel, and lightning NO are individually shut off to quantify their contributions to O_3. Simulations were conducted from August 2004 to May 2005 with the first eight months being used for initialization.

Spring in East Asia is a meteorological transition season when the winter monsoon retreats and summer monsoon gradually marches northward. Figure 3 shows the average wind vectors in the LT (~870hPa) during April-May 2005. Superimposed colors indicate the model average O_3 mixing ratios. The circulation patterns and O_3 distributions in the two simulations with GEOS-4 and GEOS-5 show similar features. In East China, the northwesterly and southwesterly winds converge around 30^o-40^oN (North China Plain), flanked by the western Pacific subtropical high to the east. In this convergence zone, surface pollutants can be readily lifted out of the boundary layer and transported to the western Pacific by westerly winds in the free troposphere (Bey et al., 2001a; Liu et al., 2003). Beijing

is located in the northern part of the North China Plain, where northwesterly winds prevail near the surface in spring. However, as the Siberian High weakens and the East Asia summer monsoon develops towards late spring, incursions of warmer tropical air from the south become more frequent and vigorous, especially in May (Ding and Chan, 2005), putting Beijing under the influence of southerly air masses.

3 Lower-tropospheric O_3 in Beijing as observed by ozonesonde and aircraft

In this section, we examine the distribution and variability of springtime lower-tropospheric O_3 in Beijing using ozonesonde and MOZAIC aircraft measurements for April-May 2005. Measurements were made by both platforms on four days: May 1, 3, 11, and 15. The vertical distributions of O_3 in the LT in the two data sets are consistent on each of these four days. This is illustrated in Figure 4 (panel a) with the four-day average profile. The consistency indicates that both ozonesonde and MOZAIC measurements well captured tropospheric O_3 concentrations over Beijing.

Figure 4 (panels b and c) shows the mean vertical distribution of O_3 below 6km as calculated from the April/May ozonesonde and aircraft data in comparison with model simulations. Model results will be discussed later in Section 4. The average O_3 distribution observed in the LT over Beijing ranged from 44 to 67 ppbv with a minimum near the surface and an enhancement at ~1.5km. Ozone concentrations remained fairly constant (~65ppbv) above ~1.5km. This LT enhancement in the vertical O_3 distribution over Beijing is consistent with the MOZAIC climatology (1995-2005) where O_3 concentrations peak below 2km in May-July, but the peak in the latter was located at a somewhat lower altitude (~1.0km) (Ding et al., 2008).

The low average O_3 concentration observed near the surface (below 1km) over Beijing (Fig. 4bc) reflects the frequent low O_3 concentrations below 1km seen in the individual sonde or aircraft profiles (Fig. 5). The minimum LT O_3 concentration seen in the ozonesonde observations was a value of 0.2 ppbv at 0.3km on May 13; on this day, O_3 mixing ratios were

lower than 2ppbv up to 0.6km. Low-O_3 episodes were also observed near the surface on Apr 17, April 23, April 29, and May 9. These low O_3 mixing ratios are likely due to the chemical titration by high NO_x concentrations, a common characteristic in urban areas (e.g., Chan, et al., 1998). Backward trajectory calculations (not shown) suggest that cleaner air masses originating from the east may also contribute to the low O_3 concentrations seen here.

The O_3 concentrations (~65 ppbv) at ~1.5 km in the average profile reflects O_3 enhancements (> 70 ppbv) frequently observed in individual profiles during April-May, 2005. Enhanced O_3 mixing ratios were observed below 4km in 15 out of total 25 days with observations: April7, April 13, April 21, April 23, April 27, April 29, May 1, May 3, May 11, May12, May 13, May 15, May 18, May 24, and May 29 (Fig. 5). Of these 15 days, 11 days (i.e., all except April 7, April 21, May 1, and May 13) saw enhanced O_3 mixing ratios at ~1.5km over Beijing. Relatively large O_3 enhancements at this altitude were mostly observed in late April and May, such as April 29, May 3, May 11, May 12, May15, May 24, and May29. The maximum O_3 concentration observed in the LT was 95 ppbv at ~1.4km on May 3 during the ozonesonde sounding campaign, and 131 ppbv at ~2.3km on May 12 as observed by MOZAIC aircraft. Ozone enhancements on May 3, May 11, and May 15 were observed simultaneously by ozonesonde and MOZAIC aircraft.

These aforementioned springtime O_3 enhancements are likely to be due to regional photochemical pollution. Recent studies indicate that transport of pollutants from surrounding regions have an important influence on air quality in Beijing during spring (Zhang et al. 2006; An et al., 2007). A regional model simulation of an air pollution episode in Beijing during April 3-7, 2005 by An et al. (2007) showed that non-Beijing sources contributed about 39% to $PM_{2.5}$ and 60% to PM_{10} concentrations in Beijing. Lin et al. (2008) showed that the North China Plain contributed 19.2 ppbv to the surface O_3 at a rural site north of Beijing (Shangdianzi, one of the regional Global Atmosphere Watch stations in China) in spring. Nevertheless, intercontinental transport may also contribute to these O_3 enhancements. We will address this issue in Section 5.

These springtime O_3 enhancements over Beijing are also likely related to favorable

meteorological conditions. LT temperature inversions were observed in sonde profiles over Beijing on April 11, April 23, April 27, April 29, May 1, May 3, May 9, May 13, and May 15 (not shown). Particularly, strong inversions were found at ~1.5km on April 29 and May 3, when relatively large O_3 enhancements were seen at the same altitude. When such inversions are present, vertical mixing is suppressed, trapping O_3 and its precursors below the inversion. This is similar to the elevated levels of O_3 previously detected above the base of temperature inversions in and nearby the similarly polluted Los Angeles Basin (Lea, 1968; Edinger, 1973; Blumenthal et al., 1978).

The LT over Beijing is near the boundary between regions of southwesterly (southerly) and northwesterly winds during spring (Fig. 3). The transition of winter-to-summer monsoon during this period has an important impact on the transport of O_3 in the LT. Trajectory classifications over Beijing during May-July, as shown by Ding et al. (2008), revealed that the O_3 concentrations in the air masses from the south are 10-15ppbv higher than those from the north below 2km, and the difference was largest at 1km. By comparing surface O_3 concentrations observed at Shangdianzi under southwest (SW) and northeast (NE) wind conditions, Lin et al. (2008) showed that the average O_3 concentrations corresponding to the SW wind directions were higher than those of NE wind directions in spring, and the difference was over 20ppbv in May. We will illustrate such influences of meteorological conditions on the LT O_3 with a case study to be presented in Section 5.

4 Model simulations of lower-tropospheric O_3 over Beijing

In this section, we present model simulations of LT O_3 over Beijing in comparison with in situ (ozonesonde and aircraft) measurements. Because the elevation of Beijing in the model is 290 meters asl, which is higher than the actual elevation (160 meters asl), there is a small gap below 290 meters where O_3 is not simulated. Figure 4bc shows the model-observation comparison of the average vertical distribution of O_3 in the LT during April-May 2005. Results from both GEOS-Chem (driven by the GEOS-4 and GEOS-5 meteorological fields)

and GMI (driven by the GEOS-4 and MERRA meteorological fields) models are shown. Figure 5 shows the time-height cross-sections of the LT O_3 mixing ratios (ppbv), as observed by ozonesonde and aircraft and simulated by GEOS-Chem during this period.

The simulated mean vertical distributions of O_3 are similar to the observations (Fig. 4bc). The GEOS-Chem/GEOS-4 model agrees with the observations near 3-4.5km, but underestimates the observations by 2 ppbv between ~1-2.5km and overestimates O_3 by 1.7-7.7ppbv below 1km and by 1.3-6.7ppbv above 4.5km, with a large bias of ~8ppbv near the surface (Fig. 4b). The GEOS-Chem/GEOS-5 simulated O_3 is in good agreement with observation above 2.5km but too low by up to 6ppbv at ~ 1-1.5km compared to observations (Fig. 4c). Both simulations showed negative biases around 1.5km, with the GEOS-Chem/GEOS-4 values in slightly better agreement. Both simulations fail to reproduce the magnitude of the daily LT O_3 enhancements over Beijing, as discussed further below.

The GMI model simulations driven by GEOS-4 and MERRA meteorological fields shown in Figure 4(bc) better reproduced than GEOS-Chem the observed values at ~0.5km. Above ~2.5km, the GMI and GEOS-Chem simulations driven by the GEOS-4 meteorology are consistent. Near 1.5km, however, GMI/GEOS-4 has a larger negative bias than GEOS-Chem (Fig. 4b). The GMI/MERRA model consistently underestimates O_3 observations below 4.5km, with the largest bias near 1.5km (~10ppbv) and larger biases than those of GEOS-Chem/GEOS-5 (Fig. 4c).

Both GEOS-Chem/GEOS-4 and GEOS-Chem/GEOS-5 simulations capture the large-scale temporal (day-to-day) variability in the vertical distribution of O_3 seen in the ozonesonde and aircraft measurements (Fig. 5). They well simulate the O_3 enhancement event at ~1.5km on May 3, which is the largest observed by both ozonesonde and MOZAIC aircraft at this altitude during this period. The timing of O_3 enhancements, especially those observed in late April and May, is reasonably captured. However, the model is missing the April 23rd enhancement and the April 27th event is shifted to April 29th in the model. Overall, the model underestimates the magnitude of those O_3 enhancements. Also, both simulations fail to reproduce the observed low-O_3 episodes near the surface, where the O_3 concentrations

are largely overestimated. Model simulations at higher horizontal resolutions that better resolve the chemical titration of O_3 by excessive NO_x may help address this discrepancy.

The distribution and variability of model relative humidity (RH) are generally similar to those observed by ozonesondes (not shown), suggesting that convective transport and large-scale ascending and descending motions in the study region are reasonably represented in the GEOS-4 and GEOS-5 meteorology. GMI/GEOS-4 and GMI/MERRA simulations also captured the observed large-scale variability in O_3 and timing of O_3 enhancements (not shown).

5 Sources of springtime O_3 enhancements in the lower troposphere over Beijing

In this section we quantify the relative contributions to the LT O_3 over Beijing of different source types and source regions in the GEOS-Chem model. We focus on model simulations driven by GEOS-4 but also discuss GEOS-Chem/GEOS-5 results where necessary. The relative contributions allow us to better understand the factors and processes contributing to the observed O_3 enhancements and distributions in the LT, and therefore may provide insights into the model limitations in the representation of chemical, physical, and dynamical processes. Figure 6 shows the major sources of the LT O_3 over Beijing during April-May 2005 as a function of date and altitude, as simulated by GEOS-Chem/GEOS-4. The plots show model results for tagged O_3 tracers transported from the stratosphere and those produced in the Asian, African, European, and North American troposphere. Figure 7 presents the changes (decreases) in the LT O_3 concentrations over Beijing when Asian, European, North American fossil fuel emissions, global biomass burning emissions, or lightning NO_x emissions were turned off, respectively, in GEOS-Chem/GEOS-4 and GEOS-Chem/GEOS-5, relative to their standard simulations. Shown in Figure 8 are the time series of temperature, total tagged O_3, and tagged O_3 tracers concentrations in the LT (~878hPa or 840-915hPa in the model) over Beijing, as simulated by GEOS-Chem/GEOS-4. These figures provide a

context for most of the discussions below.

5.1 Contributions to O_3 in the LT over Beijing of different source regions and emission types

Ozone produced within Asia made a major contribution to the LT O_3 over Beijing during April-May 2005. The Asian troposphere contributed ~10-46.6ppbv (~17-66%) in early-mid April and ~9-81ppbv (~15-88%) in late April and May (Fig. 6, top panels). The contribution was significantly higher in May than in April. This is consistent with the earlier result that relatively large enhancements of O_3, which were observed by ozonesonde and aircraft and captured in model simulations, mostly occurred in late April and May. On the dates of these O_3 enhancement events (e.g., April 29, May 3, May 13, and May 15), LT O_3 was predominantly produced within Asia (~60-79.4ppbv, or ~81%-88%). A modeling study by Sudo and Akimoto (2007) also suggested that LT O_3 in Japan and coastal China regions during TRACE-P (spring 2001) was mainly produced within Asia and mostly in the planetary boundary layer.

The aforementioned relatively large enhancements of O_3 were largely due to Asian fossil fuel emissions. When Asian fossil fuel emissions were turned off, the LT O_3 concentrations over Beijing decreased by ~3.1-21.3ppbv in the GEOS-Chem/GEOS-4 simulation and by ~3.0-25.3ppbv in the GEOS-Chem/GEOS-5 simulation in early-mid April, and decreased by ~2.2-42.4ppbv and ~3.0-37.8ppbv, respectively, in late April and May (Fig. 7, top panels). The impact of Asian fossil fuel emissions was stronger in late April and May, especially during those days with large enhancements of O_3. Without Asian fossil fuel emissions, the LT O_3 reduced by ~30-40 ppbv on April 29, May 3, May 13, and May 15. To understand the influence of fossil fuel emissions (or O_3 produced) in the sub-regions within Asia on the LT O_3 over Beijing, additional sensitivity or tagged O_3 simulations with refined emission (or O_3 source) regions would be required. Nevertheless, the case study to be presented in the following section will provide insights into the effect of regional pollution transport in this

regard.

Stratospheric contributions to the LT O_3 over Beijing during April-May 2005 were significant (Fig. 6). They were ~6.0-13.0ppbv (~8.5-20.6%) in April, and ~1.6-19.8ppbv (~2.1~23.8%) in May, and increased with altitude. On average, stratospheric contributions were larger in April (~7.6ppbv) than in May (~5.7ppbv). At the time of occurrences of the aforementioned O_3 enhancement events, stratospheric contributions were significantly reduced below ~3km (~2ppbv, ~2%). The relative magnitude of the contributions of O_3 produced within the African troposphere was lower than that of the stratospheric contributions (Fig. 6). The African troposphere contributed ~2.4-16.5ppbv (~3-28%) O_3 in April and ~0.9-10.6ppbv (~1-13%) O_3 in May.

The impact of biomass burning emissions on the LT O_3 over Beijing during this period was relatively small. When biomass burning emissions are turned off in GEOS-Chem, O_3 concentrations decrease by ~1±0.5ppbv in April and by ~2±1ppbv in May, with a maximum decrease of ~6.7ppbv on April 7 (Fig. 7). When lightning NO_x emissions are turned off, the LT O_3 concentrations fall by ~1.3-9.1 ppbv in the GEOS-Chem/GEOS-4 simulation and by ~1.5-14.5ppbv in the GEOS-Chem/GEOS-5 simulation in April; in May, they decrease by ~0.3-14.3ppbv and by ~0.5-21.3ppbv in May, respectively (Fig. 7). The larger impact of lightning NO_x emissions in May reflects the seasonal increase in continental deep convection, which results in more frequent lightning. Relatively small effects (~3±1ppbv) were seen at ~1.5km, with an effect of ~0.9±0.1ppbv O_3 at the time of large enhancements of O_3.

The European and North American source regions and their anthropogenic emissions have important impacts on LT O_3 over Beijing. Europe contributed ~2-16.7ppbv (~3-29.4%) of O_3 in April and ~2.5-20.8ppbv (~3-29.9%) in May (Fig. 6). The contributions to LT O_3 below 4km were larger in April. For these large enhancements of O_3, the contributions from Europe were significantly reduced. Similarly, North America contributed ~2.9-16.6 ppbv (~3.9-26.5%) in April and ~2.5-20.3 ppbv (3.2-26.1%) in May, with much smaller contributions during O_3 enhancement events (Fig. 6). When European fossil fuel emissions were turned off, the LT O_3 concentrations over Beijing decreased by ~1.3-10 ppbv in April and ~1-8 ppbv in May (Fig. 7).

The decreases were ~1-6 ppbv in April and ~0.6-6 ppbv in May when North American fossil fuel emissions were turned off. Again, the impacts of European and North American fossil fuel emissions were minimal (<~1ppbv) during the events of large enhancements of O_3.

Figure 8 shows the time series of total O_3, tagged O_3, and temperature in the LT (~878 hPa, ~1.5km) over Beijing in GEOS-Chem/GEOS4. Occurrences of these O_3 enhancements were accompanied by significantly increased contributions of O_3 produced in the Asian troposphere and often associated with warm air masses. On the days with relatively large observed O_3 enhancements (April 29, May 3, May13, and May 15), the contributions of O_3 from the Asian troposphere were 62.1ppbv (77.4%), 76.0ppbv (87.0%), 79.4ppbv (86.4%), and 64.0ppbv (87.2%), respectively. By contrast, at the time of these events, the contributions from Europe and North America were largely reduced. Also, compared to the more prominent contributions from the Europe (~11.6ppbv) and North America (~11.6ppbv) in early April, they were relatively smaller in late April and May, at an average of ~8.2ppbv and ~8.0ppbv, respectively.

As Beijing is located at mid-latitudes in East Asia (40°N), air masses originating from Europe and North America arrived as a result of large-scale subsidence associated with the Siberian anticyclone. Previous studies have shown that European anthropogenic emissions contribute significantly to the Asian outflow in the LT at latitudes north of 35°N (Bey et al., 2001a; Liu et al., 2003). As the Siberian high gradually weakened in spring and its center shifted westward, air masses from these regions had a reduced influence. Meanwhile, the western Pacific subtropical high developed and its center marched northwestward. As a result, the northward transport of warmer air masses from South China and along the Asian Pacific rim became more vigorous. An examination of the GEOS-4 and GEOS-5 meteorological fields shows that Beijing was mostly under the influence of southwesterly flow on the days with observed ozone enhancements. This is consistent with the stronger influence of Asian sources and more frequent occurrences of large O_3 enhancements in late April and May.

5.2 Ozone enhancements in the lower troposphere: A case study

In order to better understand the transport pathways for O_3 pollution and the vertical extent of O_3 enhancements over Beijing, we examined the largest O_3 enhancement observed by both TAPTO-China ozonesonde and MOZAIC aircraft during April-May 2005. Figure 9 shows the vertical profiles of O_3 over Beijing from TAPTO ozonesonde and MOZAIC aircraft measurements in comparison with those simulated by GEOS-Chem/GEOS-4 and GMI/GEOS-4 on May 3, 2005. Also shown are observed RH, temperature, and O_3 sources as determined by GEOS-Chem tagged O_3 and sensitivity simulations.

Ozonesonde and aircraft measurements of O_3 (0-6km) agree within ~2% on average and show similar structures in their vertical distributions. The ozone mixing ratio was lowest near the surface and increased with altitude below ~1.5km where it reached a maximum (94.7ppbv and 90ppbv in ozonesonde and aircraft measurements, respectively), and then decreased with altitude from ~1.5km to ~4km. The rapid increase of O_3 concentrations from ~1km up to ~1.5km was accompanied by a temperature inversion observed by ozonesonde. This temperature inversion inhibited the vertical mixing and transport of the air, trapping the air mass containing high levels of O_3 (and its precursors) at this level. The presence of the inversion also suggests that the high O_3 at ~1.5km was not transported from the local boundary layer via vertical mixing. Rather, backward trajectory calculations using the NOAA HYSPLIT model (Draxler and Rolph, 2014; Rolph, 2014) show that the air mass was transported downward from a higher altitude (~3km) and stayed at about 1.4km for two days before arriving at the 1.4km level over Beijing (Fig. 10).

The relatively low O_3 below 1km was likely due to chemical titration by local fresh NO_x emissions. The 5-day backward trajectory arriving at 150m over Beijing indicated that the air mass stayed near the surface during the days prior to its arrival (Fig. 10), providing optimal conditions for chemical titration.

The GEOS-Chem/GEOS-4 simulation shows an enhancement of O_3 at ~1.5km on May 3rd, but significantly underestimates its magnitude by ~10-15ppbv (Fig. 9). This is partly attributed

to the inability of a large-scale model to reproduce the local temperature inversion (not shown). The simulation reasonably reproduced the observations above 2.5km, but overestimated the observations (by ~5-10ppbv) below 1km, presumably because chemical titration was not well represented and there is too much vertical mixing due to lack of a temperature inversion in the model. The GMI/GEOS-4 simulation was better reproducing the relatively low O_3 concentrations near the surface. However, it fails to capture the O_3 enhancements at ~1.5km. The LT O_3 concentrations simulated by GMI/GEOS-4 are much lower than the observations, with the largest discrepancy (~26.9ppbv) at ~1.5km.

Model simulations suggest that this LT O_3 enhancement over Beijing was largely due to Asian fossil fuel emissions. Without Asian fossil fuel emissions in the GEOS-Chem/GEOS4 model, the simulated O_3 concentration in the LT decrease by ~30% (Fig. 9). The impact of the Asian fossil fuel emissions is largest (~30ppbv, 40%) at ~1.5km where LT O_3 concentrations reached a maximum. In addition, tagged O_3 simulations showed that 79.6% of O_3 at ~1.5km originated from the Asian troposphere (not shown). When lightning NO_x emissions were suppressed, the decreases of the LT O_3 over Beijing increased with altitude, with the smallest decreases (~1.2ppbv, ~1.7%) below ~1.5km. Similarly, the contributions of stratospheric O_3 increased with altitude, with a small contribution (~2.9ppbv, ~4%) at ~1.5km where the largest enhancement of O_3 occurred. Therefore, this LT O_3 enhancement was mainly due to the regional anthropogenic pollution within Asia.

The GEOS4 assimilated meteorological data driving the GEOS-Chem model indicate that strong southwesterly winds prevailed over Beijing in the LT on May 2-3 (Fig. 11, Fig. 12). Meanwhile, a low-pressure center in the LT at (~43°-53°N, 120°-140°E) put the area north of Beijing under the influence of northwesterly winds. The southwesterly and northwesterly winds met just north of Beijing at around 43°N, forming a convergence zone. As part of the western Pacific subtropical high developing around 15°-30°N, strong southwesterly winds over southern and eastern China could have readily swept the pollutants in its pathway into Beijing. Indeed, an area of high CO (>200ppbv) was located to the southwest of the North China Plain on May 2-3 at 878hPa. The air mass stayed in this high CO area for a couple of

days before arriving at 1.4km over Beijing (Fig. 10), where the O_3 enhancement was observed by both sonde and aircraft, as well as simulated by the model. By contrast, the air mass arriving at 2.4km came straight from the west where air was cleaner and thus had significantly lower O_3. The high CO area was largest near the surface and became smaller with altitude. High CO concentrations were seen in the model simulations up to ~797hPa. No high-CO plumes were found at ~704hPa over East Asia on May 2-3 in the model (not shown). By May 3, Beijing was at the center of the high O_3 area (>72ppbv) in the LT (797hPa and 878hPa, Fig. 12) on May 3. The O_3 concentrations were also relatively lower (~68±4ppbv) near the surface (942hPa) and at a higher altitude (704hPa).

6 Summary and conclusions

We have characterized the vertical distribution of lower-tropospheric O_3 over Beijing using observations from 16 ozonesonde soundings made during the TAPTO-China field campaign in April-May 2005, as well as MOZAIC aircraft ascending and descending profiles over 13 days in this period. A particular focus was placed on the origin of O_3 enhancements in the lower troposphere (LT, 0-6km). We used a global 3-D chemistry and transport model (GEOS-Chem CTM) driven by assimilated meteorological fields from the NASA Goddard Earth Observing System (GEOS-4 and GEOS-5) to interpret these characteristics and quantify the sources contributing to O_3 and its enhancements in the springtime LT over Beijing. We also used the output of the Global Modeling Initiative (GMI) CTM for comparison with O_3 observations.

The average observed profile of O_3 mixing ratio in the LT over Beijing during April-May, 2005 ranged from ~44 to 67ppbv with an enhancement at the altitude of ~1.5km and a relatively low abundance near the surface. The relatively high average O_3 concentrations at ~1.5 km were due to frequently observed elevated O_3 levels (up to 94.7 ppbv in soundings and 130.3ppbv in MOZAIC aircraft measurements). Such enhancements were observed at this altitude in 15 out of 25 days with observations during this period. Ozone enhancements

were more frequently observed by ozonesonde in late April and May relative to early and mid- April. This relates to northward transport of pollution in East China to the LT over Beijing due to weakening of the Siberian high and the onset of the Asian summer monsoon. It also suggests that an earlier onset of the Asian summer monsoon would cause more O_3 enhancement events in the LT over the North China Plain in late spring and early summer.

The GEOS-Chem model driven by GEOS-4 and GEOS-5 assimilated meteorological fields adequately reproduced the average vertical distribution of LT O_3 and captured the timing of the observed O_3 enhancement events over Beijing during April-May 2005, but both simulations underestimated the magnitude of these enhancements. On the other hand, GEOS-Chem overestimated the observed low O_3 concentrations near the surface. The GMI model driven by GEOS-4 and MERRA better resolved the average O_3 concentrations near the surface, but was less successful in reproducing the enhancement of average O_3 concentrations at ~1.5km. Nevertheless, GMI did capture the timing of the major O_3 enhancement events observed. Both GEOS-Chem and GMI were successful in reproducing temporal fluctuations of observed O_3 because they are driven by assimilated meteorological fields. The fact that they did not capture the surface low or the 1.5km peak likely resulted from a combination of inability to represent the chemical regime at the surface (i.e., NOx-driven titration) due to low spatial resolution, and overly vigorous vertical transport (i.e., lack of a temperature inversion at the altitude of ~1.5km).

We investigated the sources contributing to the LT O_3 enhancements observed over Beijing during April-May 2005 by tagging O_3 produced in different source regions in the GEOS-Chem/GEOS-4 model and by conducting model sensitivity calculations. We found that these O_3 enhancements were predominantly attributed to O_3 produced within Asia, especially for relatively large enhancements (~81~88%). For the large enhancements, the O_3 concentrations at ~1.5km were reduced by ~30-40ppbv when Asian fossil fuel emissions were suppressed within the model. Contributions of O_3 from outside Asia were relatively small during these O_3 events. However, long-range transport of O_3 (and its precursors) from Europe and North America has important impacts on LT O_3 over Beijing during non-event

periods, especially in April. The two alternating regimes of transport reflect the springtime transition from winter to summer monsoon in East Asia.

A case study of the O_3 enhancements at ~1.5km observed on May 3, 2005 showed that the event was largely attributed to Asian fossil fuel emissions (34%). Backward trajectory calculations suggested that the air mass stayed in the LT to the southwest of Beijing for a couple of days before arriving at ~1.4km over Beijing. Elevated CO levels were found in the model results on May 2nd and 3rd in the area where the air mass remained before reaching Beijing. The model simulations showed that Beijing was at the center of the high O_3 area in the LT (~878hPa to 797hPa) by May 3, with prevailing strong southwesterly winds that swept O_3 and its precursors downwind to Beijing.

We find that the ozonesonde and aircraft observations of springtime O_3 in the LT over Beijing are qualitatively consistent with the current understanding of tropospheric chemistry and transport as represented by the GEOS-Chem model. Using the same model driven by different meteorological fields (GEOS-4 and GEOS-5) does not alter our conclusion. However, current global models (e.g., GEOS-Chem and GMI) have difficulty in quantitatively reproducing the observed enhancements and depletions of the LT O_3 over Beijing. Model simulations at higher resolutions would better resolve regional meteorology and transport with respect to the topography in the North China Plain, and chemical transformation such as the titration of O_3 by NO. Models could also be further evaluated by increasing satellite observations as well as multi-year ozonesonde (Wang et al., 2012) and aircraft measurements (Ding et al., 2008). Such efforts would improve our quantitative understanding of the origin of tropospheric O_3 and elevated O_3 events over the North China Plain, allowing a better projection of regional O_3 pollution and its global impact.

Appendix A: GEOS-Chem CTM

An earlier version of the GEOS-Chem model that we applied to the analysis of ozonesonde O_3 observations was described in the appendix of Zhang et al. (2012). A similar

description is included here for completeness, but for version v9-01-02 and with a different configuration. We drive the GEOS-Chem model with the GEOS-4 and GEOS-5 assimilated meteorological observations from the Goddard Earth Observing System (GEOS) of the NASA Global Modeling and Assimilation Office (GMAO). The original description and evaluation of GEOS-Chem as applied to tropospheric O_3-NO_x-VOC chemistry was presented by Bey et al. (2001a) and a description of the coupled oxidant-aerosol simulation was given by Park et al. (2004). A number of previous studies have applied the model to tropospheric O_3 in various regions of the world, including the Asian and western Pacific (e.g., Bey et al., 2001b; Liu et al., 2002), the Middle East (e.g., Li et al., 2001; Liu et al., 2009), the United States (e.g., Fiore et al., 2002; Zhang et al., 2008; Hudman et al., 2009), the Atlantic (e.g., Li et al., 2002), and the tropics (e.g., Martin et al., 2002; Nassar et al., 2009; Zhang et al., 2011).

The temporal resolution of the GEOS-4 and GEOS-5 meteorological data is 6 hours (3 hours for surface variables and mixing depth). GEOS-4 has a native resolution of 1° latitude by 1.25° longitude with 55 vertical levels between surface and 0.01hPa and 8 vertical levels between 0-6km. GEOS-5 has a higher native resolution of 0.5° latitude by 0.667° longitude with 72 levels in the vertical and 23 vertical levels between 0-6km. For computational expediency, horizontal resolutions are degraded to 2° latitude by 2.5° longitude for input to GEOS-Chem. In addition, vertical levels above 50hPa (GEOS-4) or 80hPa (GEOS-5) are merged to retain 30 (GEOS-4) or 47 (GEOS-5) vertical levels in total. A major difference between GEOS-4 and GEOS-5 is the parameterization scheme for convection. GEOS-4 uses the parameterization scheme of Zhang and McFarlane (1995) and Hack (1994) for deep convection and shallow convection, respectively. Convection in GEOS-5 is based on the relaxed Arakawa-Schubert parameterization scheme (Moorthi and Suarez, 1992). Previous model simulations of ^{222}Rn (Zhang et al., 2011) and CO (Liu et al., 2010) indicate that tropical deep convection is significantly deeper in GEOS-4 than in GEOS-5. GEOS-Chem assumes rapid vertical mixing within the mixing layers diagnosed by GEOS.

The GEOS-Chem model includes 87 chemical species and transports 43 chemical tracers to describe tropospheric O_3-NO_x-VOCs-aerosol chemistry. Anthropogenic emissions are

based on the Global Emission Inventory Activity (GEIA) (Benkovitz et al., 1996), overwritten with NO_x, CO and SO_x from the Emission Database for Global Atmospheric Research (EDGAR) inventory (Olivier and Berdowski, 2001) and from various regional emissions inventories as described by Nassar et al. (2009). Anthropogenic emissions in Asia are from the Streets 2000 inventory (Streets et al., 2003), with anthropogenic CO emissions in China updated by the Streets 2001 inventory (Streets et al., 2006). These base inventory emissions are scaled to our 2005 simulation year, following van Donkelaar et al. (2008). The 2005 anthropogenic emission for Asia (0–60°N, 65–150°E) is 10.1 Tg N/yr for NO_x and 271.9 Tg/yr for CO. Biofuel emissions follow Yevich and Logan (2003). Biogenic VOCs emissions are based on the Model of Emissions of Gases and Aerosol from Nature (MEGAN) inventory (Guenther et al., 2006). Biomass burning emissions are based on the Global Fire Emissions Database version 2 (GFEDv2), which resolves interannual variability (van der Werf et al., 2006). The monthly GFEDv2 emissions were resampled to an 8-day time step using MODIS fire hot spots (Giglio et al., 2003; Nassar et al., 2009).

Lightning NO emissions in GEOS-Chem are calculated locally in deep convection events with the scheme of Price and Rind (1992) that links flash rates to convective cloud top heights. The spatial distribution of lightning averaged over 11 years in the model is constrained to match the climatological (11-year) satellite observations of lightning flash rates from the Optical Transient Detector / Lightning Imaging Sensor (OTD-LIS) High Resolution Monthly Climatology (HRMC v2.2) product by applying a local monthly rescaling factor (Sauvage et al., 2007; Nassaret al., 2009). The interannual variability of the lightning NO_x emissions as represented by the model is retained, with approximately 6 Tg N yr^{-1} released globally (Sauvage et al., 2007; Nassar et al., 2009). The vertical distribution of lightning NO_x emissions follows Pickering et al. (1998), with most of NO_x in the upper troposphere (55–75% above 8 km). The model uses the linearized stratospheric O_3 chemistry scheme (Linoz) of McLinden et al. (2000). Liu et al. (2015) previously suggested that Linoz in a CTM driven with the GEOS-4 and GEOS-5 assimilated meteorological fields yields reasonable impacts of cross-tropopause transport on the lower troposphere.

Acknowledgements

This work was supported by NASA Atmospheric Composition Modeling and Analysis Program (ACMAP) and NASA Modeling, Analysis, and Prediction Program (MAP). Ozonesonde data were obtained with support from the National Science Foundation of China. We thank the personnel at the Beijing ozonesonde station for helping with the launching of ozonesondes. The authors acknowledge the strong support of the European Commission, Airbus, and the Airlines (Lufthansa, Air-France, Austrian, Air Namibia, China Airlines, and Cathay Pacific so far) who carry the MOZAIC or IAGOS equipment and perform the maintenance since 1994. MOZAIC is presently funded by INSU-CNRS (France), Météo-France, CNES, Université Paul Sabatier (Toulouse, France) and Research Center Jülich (FZJ, Jülich, Germany). IAGOS has been and is additionally funded by the EU projects IAGOS-DS and IAGOS-ERI. The MOZAIC-IAGOS data are available via CNES/CNRS-INSU Ether web site http://www.pole-ether.fr. NASA Center for Computational Sciences (NCCS) provided supercomputing resources. The GEOS-Chem model is managed by the Atmospheric Chemistry Modeling Group at Harvard University with support from NASA ACMAP and MAP. The GMI model is managed by Dr. Jose Rodriguez (Project Scientist) and Dr. Susan Strahan (Project Manager) at NASA Goddard Space Flight Center with support from MAP. We thank Meiyun Lin and two anonymous reviewers for their comments and suggestions, which helped improve the manuscript.

References

Allen, D., Pickering, K., Duncan, B., and Damon, M.: Impact of lightning NO emissions on North American photochemistry as determined using the Global Modeling Initiative (GMI) model, J. Geophys. Res., 115, D22301, doi:10.1029/2010JD014062, 2010.

An, X., Zhu, T., Wang, Z., Li, C., and Wang, Y.: A modeling analysis of a heavy air pollution episode occurred in Beijing, Atmos. Chem. Phys., 7, 3103-3114,

doi:10.5194/acp-7-3103-2007, 2007.

Benkovitz, C. M., Scholtz, M. T., Pacyna, J., Tarrason, L., Dignon, J., Voldner, E. C., Spiro, P. A., Logan, J. A., and Graedel, T. E.: Global gridded inventories of anthropogenic emissions of sulfur and nitrogen, J. Geophys. Res., 101, D22, 29,239–29,253, doi:10.1029/96JD00126, 1996.

Bey, I., Jacob, D. J., Logan, J. A., and Yantosca, R. M.: Asian chemical outflow to the Pacific in spring: Origins, pathways, and budgets, J. Geophys. Res., 106, D19, 23097-23113, doi:10.1029/2001JD000806, 2001a.

Bey, I., Jacob, D. J., Yantosca, R. M., Logan, J. A., Field, B. D., Fiore, A. M., Li, Q., and Liu, H., Mickley, L.J., and Schultz, M.G.: Global modeling of tropospheric chemistry with assimilated meteorology: Model description and evaluation, J. Geophys. Res., 106, D19, 23073-23095, doi:10.1029/2001JD000807, 2001b.

Bloom, S., da Silva, A., Dee, D. Bosilovich, M., Chern, J., Pawson, S., Schubert, S., Sienkiewicz, M., Stajner, I., and Tan, W.-W., and Wu, M.-L.: Documentation and validation of the Goddard Earth Observing System (GEOS) data assimilation system-Version 4, Technical Report Series on Global Modeling and Data Assimilation, Vo. 26, No. NASA/TM-2005-104606, Greenbelt, Maryland, U.S.A., 2005.

Blumenthal, D., White, W., and Smith, T.: Anatomy of a Los Angeles smog episode: Pollutant transport in the daytime sea breeze regime, Atmos. Environ., 15, 893-907, 1978.

Chan, C., Chan, L., and Harris, J.: Urban and background ozone trend in 1984-1999 at subtropical Hong Kong, South China, Ozone-Sci. Eng., 25, 513-522, 2003.

Chan, C., Li, Y., Tang, J., Leung, Y., Wu, M., Chan, L., Chang, C., and Liu, S.: An analysis on abnormally low ozone in the upper troposphere over subtropical East Asia in spring 2004, Atmos. Environ., 41, 3556–3564, 2007.

Chan, L.Y., Liu, H.Y., Lam, K.S., Wang, T., Oltmans, S.J., and Harris, J.M.: Analysis of the seasonal behavior of tropospheric ozone at Hong Kong, Atmos. Environ., 32(2), 159-168,

1998.

Considine, D. B., Logan, J. A., and Olsen, M. A.: Evaluation of near-tropopause ozone distributions in the Global Modeling Initiative combined stratosphere/troposphere model with ozonesonde data, Atmos. Chem. Phys., 8, 2365-2385, doi:10.5194/acp-8-2365-2008, 2008.

Cooper, O. R., Parrish, D. D., Stohl, A., Trainer, M., Nedelec, P., Thouret, V., Cammas, J., Oltmans, S. J., Johnson, B. J., Tarasick, D., Leblanc, T., McDermid, I. S., Jaffe, D., Gao, R., Stith, J., Ryerson, T., Aikin, K., Campos, T., Weinheimer, A. J., and Avery, M.A.: Increasing springtime ozone mixing ratios in the free troposphere over western North America, Nature, 463, 344-348, doi:10.1038/nature08708, 2010.

Ding, Y., and Chan, J. C. L.: The East Asian summer monsoon: An overview, Meteorol. Atmos. Phys., 89, 117–142, doi:10.1007/s00703-005-0125-z, 2005.

Ding, A., Wang, T., Thouret, V., Cammas, J. P., and Nédélec, P.: Tropospheric ozone climatology over Beijing: analysis of aircraft data from the MOZAIC program, Atmos. Chem. Phys., 8, 1-13, doi:10.5194/acp-8-1-2008, 2008.

Doughty, D. C., Thompson, A. M., Schoeberl, M. R., Stajner, I., Wargan, K., and Hui, W. C. J.: An intercomparison of tropospheric ozone retrievals derived from two Aura instruments and measurements in western North America in 2006, J. Geophys. Res., 116, D06303, doi:10.1029/2010JD014703, 2011.

Draxler, R.R. and Rolph, G.D.,: HYSPLIT (HYbrid Single-Particle Lagrangian Integrated Trajectory) Model access via NOAA ARL READY Website (http://ready.arl.noaa.gov/HYSPLIT.php), NOAA Air Resources Laboratory, Silver Spring, MD, 2014.

Dufour, G., Eremenko, M., Orphal, J., and Flaud, J.-M: IASI observations of seasonal and day-to-day variations of tropospheric ozone over three highly populated areas of China: Beijing, Shanghai, and Hong Kong, Atmos. Chem. Phys., 10, 3787-3801, doi:10.5194/acp-10-3787-2010, 2010.

Duncan, B. N., Strahan, S. E., Yoshida, Y., Steenrod, S. D., and Livesey, N.: Model study of the cross-tropopause transport of biomass burning pollution, Atmos. Chem. Phys., 7, 3713-3736, doi:10.5194/acp-7-3713-2007, 2007.

Edinger, J. G.: Vertical distribution of photochemical smog in Los Angeles basin, Environ. Sci. Technol., 7, 247–252, doi:10.1021/es60075a004, 1973.

Fiore, A. M., Jacob, D. J., Bey, I., Yantosca, R. M., Field, B. D., Fusco, A. C., and Wilkinson, J. G.: Background ozone over the United States: Implications for air quality policy, J. Geophys. Res., 107(D15), 4275, doi:10.1029/2001JD000982, 2002.

Fu, T.-M., Jacob, D. J., Palmer, P. I., Chance, K., Wang, Y. X., Barletta, B., Blake, D. R., Stanton, J. C., and Pilling, M. J.: Space-based formaldehyde measurements as constraints on volatile organic compound emissions in east and south Asia and implications for ozone, J. Geophys. Res., 112, D06312, doi:10.1029/2006JD007853, 2007.

Giglio, L., Descloitres, J., Justice, C. O., and Kaufman, Y. J.: An enhanced contextual fire detection algorithm for MODIS, Remote Sens. Environ., 87, 273–282, doi:10.1016/S0034-4257(03)00184-6, 2003.

Guenther, A., Karl, T., Harley, P., Wiedinmyer, C., Palmer, P. I., and Geron, C.: Estimates of global terrestrial isoprene emissions using MEGAN (Model of Emissions of Gases and Aerosols from Nature), Atmos. Chem. Phys., 6, 3181–3210, doi:10.5194/acp-6-3181-2006, 2006.

Hack, J. J.: Parameterization of moist convection in the National Center for Atmospheric Research community climate model (CCM2), J. Geophys. Res., 99(D3), 5551–5568, doi:10.1029/93JD03478, 1994.

Hudman, R. C., Murray, L. T., Jacob, D. J., Turquety, S., Wu, S., Millet, D. B., Avery, M., Goldstein, A. H., and Holloway, J.: North American influence on tropospheric ozone and the effects of recent emission reductions: Constraints from ICARTT observations, J. Geophys. Res., 114, D07302, doi:10.1029/2008JD010126, 2009.

Hudman, R. C., Jacob, D. J., Cooper, O. R., Evans, M. J., Heald, C. L., Park, R. J., Fehsenfeld, F., Flocke, F., Holloway, J., Hubler, G., Kita, K., Koike, M., Kondo, Y., Neuman, A., Nowak, J., Oltmans, S., Parrish, D., Roberts, J. M., and Ryerson, T.: Ozone production in transpacific Asian pollution plumes and implications for ozone air quality in California, J. Geophys. Res., 109, D23S10, doi:10.1029/2004JD004974, 2004.

Jaffe, D., Anderson, T., Covert, D., Kotchenruther, R., Trost, B., Danielson, J., Simpson, W., Berntsen, T., Karlsdottir, S., and Blake, D.: Transport of Asian air pollution to North America, Geophys. Res. Lett., 26(6), 711–714, doi:10.1029/1999GL900100, 1999.

Lacis, A. A., Wuebbles, D. J., and Logan, J. A.: Radiative forcing of climate by changes in the vertical distribution of ozone, J. Geophys. Res., 95(D7), 9971–9981, doi:10.1029/JD095iD07p09971, 1990.

Lea, D. A.: Vertical ozone distribution in the lower troposphere near an urban pollution complex, J. Appl. Met., 7, 252–267, 1968.

Lee, S. H., Akimoto, H., Nakane, H., Kurnosenko, S., and Kinjo, Y.: Lower tropospheric ozone trend observed in 1989-1997 at Okinawa, Japan, Geophys. Res.Lett., 25(10), 1637-1640, 1998.

Li, Q., Jacob, D. J., Logan, J. A., Bey, I., Yantosca, R. M., Liu, H. Y., Martin, R. V., Fiore, A. M., Field, B. D., and Duncan, B. N.:A tropospheric ozone maximum over the Middle East, Geophys. Res. Lett., 28, 3235–3238, doi:10.1029/2001GL013134, 2001.

Li, Q., Jacob, D. J., Fairlie, T. D., Liu, H., Martin, R. V., and Yantosca, R. M.: Stratospheric versus pollution influences on ozone at Bermuda: Reconciling past analyses, J. Geophys. Res., 107(D22), 4611, doi:10.1029/2002JD002138, 2002.

Liang, Q., Jaeglé, L., Jaffe, D. A., Weiss-Penzias, P., Heckman, A., and Snow, J. A.: Long-range transport of Asian pollution to the northeast Pacific: Seasonal variations and transport pathways of carbon monoxide, J. Geophys. Res., 109, D23S07, doi:10.1029/2003JD004402, 2004.

Lin, W., Xu, X., Zhang, X., and Tang, J.: Contributions of pollutants from North China Plain to surface ozone at the Shangdianzi GAW Station, Atmos. Chem. Phys., 8, 5889-5898, doi:10.5194/acp-8-5889-2008, 2008.

Lin, M., Holloway, T., Oki, T., Streets, D. G., and Richter, A.: Multi-scale model analysis of boundary layer ozone over East Asia, Atmos. Chem. Phys., 9, 3277-3301, doi:10.5194/acp-9-3277-2009, 2009.

Lin, M., Fiore, A. M., Horowitz, L. W., Cooper, O. R., Naik, V., Holloway, J., Johnson, B. J., Middlebrook, A. M., Oltmans, S. J., Pollack, I. B., Ryerson, T. B., Warner, J. X., Wiedinmyer, C., Wilson, J., and Wyman, B.: Transport of Asian ozone pollution into surface air over the western United States in spring , J. Geophys. Res., 117, D00V07, doi:10.1029/2011JD016961, 2012.

Lin, M., Horowitz, L. W., Oltmans, S. J., Fiore, A. M., and Fan, S.: Tropospheric ozone trends at Manna Loa Observatory tied to decadal climate variability, Nature Geoscience, 7, 136-143, doi:10.1038/NGEO2066, 2014.

Liu, H., Chang, W. L., Oltmans, S. J., Chan, L. Y., and Harris, J. M.: On springtime high ozone events in the lower troposphere from southeast Asian biomass burning, Atmos. Environ., 33(15), 2403-2410, 1999.

Liu, H., Jacob, D. J., Chan, L. Y., Oltmans, S. J., Bey, I., Yantosca, R. M., Harris, J. M., Duncan, B. N., and Martin, R. V.: Sources of tropospheric ozone along the Asian Pacific Rim: An analysis of ozonesonde observations, J. Geophys. Res., 107(D21), 4573, doi:10.1029/2001JD002005, 2002.

Liu, H., Jacob, D. J., Bey, I., Yantosca, R. M., Duncan, B. N., and Sachse, G. W.: Transport pathways for Asian pollution outflow over the Pacific: Interannual and seasonal variations, J. Geophys. Res., 108, 8786, doi:10.1029/2002JD003102, D20, 2003.

Liu H., Considine, D. B., Horowitz, L. W., Crawford, J. H., Strahan, S. E., Damon, M., Rodriguez, J. M., Xu, X., Carouge, C. C., and Yantosca, R. M.: Using beryllium-7 to assess cross-tropopause transport in global models, Atmos. Chem. Phys., to be submitted,

2015.

Liu, J. J., Jones, D. B. A., Worden, J. R., Noone, D., Parrington, M., and Kar, J.,: Analysis of the summertime buildup of tropospheric ozone abundances over the Middle East and North Africa as observed by the Tropospheric Emission Spectrometer instrument, J. Geophys. Res., 114, D05304, doi:10.1029/2008JD010993, 2009.

Liu, J., Logan, J., Jones, D., Livesey, N., Megretskaia, I., Carouge, C., and Nedelec, P. Analysis of CO in the tropical troposphere using Aura satellite data and the GEOS-Chem model: Insights into transport characteristics of the GEOS meteorological products, Atmos. Chem. Phys., 10, 12207-12232, doi:10.5194/acp-10-12207-2010, 2010.

Marenco, A., Thouret, V., Nédélec, P., Smit, H., Helten, M., Kley, D., Karcher, F., Simon, P., Law, K., and Pyle, J.: Measurement of ozone and water vapor by Airbus in-service aircraft: The MOZAIC airborne program, an overview, J. Geophys. Res., 103(D19), 25631–25642, doi:10.1029/98JD00977, 1998.

Martin, R.V., Jacob, D.J., Logan, J.A., Bey I., Yantosca, R.M., Staudt, A.C., Li, Q., Fiore, A.M., Duncan, B.N., Liu, H., Ginoux, P., and Thouret, V.: Interpretation of TOMS observations of tropical tropospheric ozone with a global model and in-situ observations, J. Geophys. Res., 107(D18), 4351, doi:10.1029/2001JD001480, 2002.

McLinden, C. A., Olsen, S. C., Hannegan, B., Wild, O., Prather, M. J., and Sundet, J.: Stratospheric ozone in 3-D models: A simple chemistry and the cross-tropopause flux, J. Geophys. Res., 105, 14,653–14,665, doi:10.1029/2000JD900124, 2000.

Moody, J. L., Felker, S. R., Wimmers, A. J., Osterman, G., Bowman, K., Thompson, A. M., and Tarasick, D. W.: A multi-sensor upper tropospheric ozone product (MUTOP) based on TES ozone and GOES water vapor: validation with ozonesondes, Atmos. Chem. Phys., 12, 5661-5676, doi:10.5194/acp-12-5661-2012, 2012.

Moorthi, S., and Suarez, M.: Relaxed Arakawa-Schubert: A parameterization of moist convection for general circulation models, Mon. Wea. Rev., 120, 978-1002, 1992.

Nassar, R., Logan, J. A., Megretskaia, I. A., Murray, L. T., Zhang, L., and Jones D. B. A.: Analysis of tropical tropospheric ozone, carbon monoxide, and water vapor during the 2006 El Niño using TES observations and the GEOS-Chem model, J. Geophys. Res., 114, D17304, doi:10.1029/2009JD011760, 2009.

Olivier, J. G. J., and Berdowski, J. J. M.: Global emissions source and sinks, in The Climate System, edited by J. Berdowski, R. Guicherit, and B. J. Heji, pp. 33–78, A. A. Balkema, Lisse, Netherlands, 2001.

Park, R. J., Jacob, D. J., Field, B. D., Yantosca, R. M., and Chin, M.: Natural and transboundary pollution influences on sulfate-nitrate-ammonium aerosols in the United States: Implications for policy, J. Geophys. Res., 109, D15204, doi:10.1029/2003JD004473, 2004.

Pickering, K. E., Wang, Y., Tao, W.-K., Price, C., and Müller, J.-F.: Vertical distributions of lightning NO_x for use in regional and global chemical transport models, J. Geophys. Res., 103, 31,203–31,216, doi:10.1029/98JD02651, 1998.

Price, C., and Rind, D.: A simple lightning parameterization for calculating global lightning distributions, J. Geophys. Res., 97, 9919–9933, doi:10.1029/92JD00719, 1992.

Richter, A., Burrows, J. P., Nüß, H., Granier, C., and Niemeier, U.: Increase in tropospheric nitrogen dioxide over China observed from space, Nature, 437, 129–132, doi:10.1038/nature04092, 2005.

Rienecker, M. M., Suarez, M. J., Todling, R., Bacmeister, J., Takacs, L., Liu, H.-C., Gu, W., Sienkiewicz, M., Koster, R. D., Gelaro, R., Stajner, I., and Nielsen, J. E.: The GEOS-5 Data Assimilation System - Documentation of Versions 5.0.1, 5.1.0, and 5.2.0. Tech. Rep. NASA-TM-104606, Technical Report Series on Global Modeling and Data Assimilation, Vol. 27, 101pp, Greenbelt, Maryland, U.S.A., 2008.

Rolph, G. D.: Real-time Environmental Applications and Display sYstem (READY) Website (http://ready.arl.noaa.gov). NOAA Air Resources Laboratory, Silver Spring, MD, 2014.

Sauvage, B., Martin, R. V., van Donkelaar, A., Liu, X., Chance, K., Jaeglé, L., Palmer, P. I., Wu, S., and Fu, T.-M.: Remote sensed and in situ constraints on processes affecting tropical tropospheric ozone, Atmos. Chem. Phys., 7, 815–838, doi:10.5194/acp-7-815-2007, 2007.

Strahan, S. E., Duncan, B. N., and Hoor, P.: Observationally derived transport diagnostics for the lowermost stratosphere and their application to the GMI chemistry and transport model, Atmos. Chem. Phys., 7, 2435-2445, doi:10.5194/acp-7-2435-2007, 2007.

Streets, D. G., Bond, T., Carmichael, G., Fernandes, S., Fu, Q., He, D., Klimont, Z., Nelson, S., Tsai, N., and Wang, M. Q.: An inventory of gaseous and primary aerosol emissions in Asia in the year 2000, J. Geophys. Res., 108, 8809, doi:10.1029/2002JD003093, D21, 2003.

Streets, D. G., Zhang, Q., Wang, L., He, K., Hao, J., Wu, Y., Tang, Y., and. Carmichael, G. R.: Revisiting China's CO emissions after the Transport and Chemical Evolution over the Pacific (TRACE-P) mission: Synthesis of inventories, atmospheric modeling, and observations, J. Geophys. Res., 111, D14306, doi:10.1029/2006JD007118, 2006.

Streets, D. G., Fu, J. S., Jang, C. J., Hao, J., He, K., Tang, X., Zhang, Y., Wang, Z., Li, Z., and Zhang, Q.: Air quality during the 2008 Beijing Olympic games, Atmos. Environ., 41(3), 480-492, 2007.

Sudo, K., and Akimoto, H.: Global source attribution of tropospheric ozone: Long-range transport from various source regions, J. Geophys. Res., 112, D12302, doi:10.1029/2006JD007992, 2007.

Thompson, A. M.: The oxidizing capacity of the earth's atmosphere: Probable past and future changes, Science, 256, 1157– 1165, 1992.

Thouret, V., Marenco, A., Nédélec, P., and Grouhel, C.: Ozone climatologies at 9–12 km altitude as seen by the MOZAIC airborne program between September 1994 and August 1996, J. Geophys. Res., 103(D19), 25653–25679, doi:10.1029/98JD01807, 1998.

Thouret, V., Cammas, J. P., Sauvage, B., Athier, G., Zbinden, R., Nédélec, P., Simon, P., and Karcher, F.: Tropopause referenced ozone climatology and inter-annual variability (1994–2003) from the MOZAIC programme, Atmos. Chem. Phys., 6, 1033-1051, doi:10.5194/acp-6-1033-2006, 2006.

van der Werf, G. R., Randerson, J. T., Giglio, L., Collatz, G. J., Kasibhatla, P. S., and Arellano Jr., A. F.: Interannual variability in global biomass burning emissions from 1997 to 2004, Atmos. Chem. Phys., 6, 3423–3441, doi:10.5194/acp-6-3423-2006, 2006.

van Donkelaar, A., Martin, R. V., Leaitch, W. R., Macdonald, A. M., Walker, T. W., Streets, D. G., Zhang, Q., Dunlea, E. J., Jimenez, J. L., Dibb, J. E., Huey, L. G., Weber, R., and Andreae, M. O.: Analysis of aircraft and satellite measurements from the Intercontinental Chemical Transport Experiment (INTEX-B) to quantify long-range transport of East Asian sulfur to Canada, Atmos. Chem. Phys., 8, 2999–3014, doi:10.5194/acp-8-2999-2008, 2008.

Wang, Y., Jacob, D. J., and Logan, J. A.: Global simulation of tropospheric O_3-NO_x-hydrocarbon chemistry: 3. Origin of tropospheric ozone and effects of nonmethane hydrocarbons, J. Geophys. Res., 103(D9), 10757–10767, doi:10.1029/98JD00156, 1998.

Wang, T., Ding, A., Gao, J., and Wu, W. S.: Strong ozone production in urban plumes from Beijing, China, Geophys. Res. Lett., 33, L21806, doi:10.1029/2006GL027689, 2006.

Wang, Y., McElroy, M. B., Munger, J. W., Hao, J., Ma, H., Nielsen, C. P., and Chen, Y.: Variations of O_3 and CO in summertime at a rural site near Beijing, Atmos. Chem. Phys., 8, 6355-6363, doi:10.5194/acp-8-6355-2008, 2008.

Wang, T., Wei, X., Ding, A., Poon, C., Lam, K., Li, Y., Chan, L., and Anson, M.: Increasing surface ozone concentrations in the background atmosphere of Southern China, 1994-2007, Atmos. Chem. Phys., 9, 6217-6227, doi:10.5194/acp-9-6217-2009, 2009.

Wang, Y., Konopka, P., Liu, Y., Chen, H., Müller, R., Plöger, F., Riese, M., Cai, Z., and Lü, D.: Tropospheric ozone trend over Beijing from 2002–2010: Ozonesonde measurements

and modeling analysis, Atmos. Chem. Phys., 12, 8389-8399, doi:10.5194/acp-12-8389-2012, 2012.

Yevich, R., and Logan, J. A.: An assessment of biofuel use and burning of agricultural waste in the developing world, Global Biogeochem. Cycles, 17(4), 1095, doi:10.1029/2002GB001952, 2003.

Zbinden, R. M., Thouret, V., Ricaud, P., Carminati, F., Cammas, J.-P., and Nédélec, P.: Climatology of pure tropospheric profiles and column contents of ozone and carbon monoxide using MOZAIC in the mid-northern latitudes (24°N to 50°N) from 1994 to 2009, Atmos. Chem. Phys., 13, 12363-12388, doi:10.5194/acp-13-12363-2013, 2013.

Zhang, G. J., and McFarlane, N. A.: Sensitivity of climate simulations to the parameterization of cumulus convection in the Canadian Climate Centre general circulation model, Atmosphere-Ocean, 33(3), 407-446, 1995.

Zhang, Q., Zhao, C., Tie, X., Wei, Q., Huang, M., Li, G., Ying, Z., and Li, C.: Characterizations of aerosols over the Beijing region: A case study of aircraft measurements, Atmos. Environ., 40, 4513-4527, doi:10.1016/j.atmosenv.2006.04.032, 2006.

Zhang, L., Jacob, D. J., Boersma, K. F., Jaffe, D. A., Olson, J. R., Bowman, K. W., Worden, J. R., Thompson, A. M., Avery, M. A., Cohen, R. C., Dibb, J. E., Flock, F. M., Fuelberg, H. E., Huey, L. G., McMillan, W. W., Singh, H. B., and Weinheimer, A. J.: Transpacific transport of ozone pollution and the effect of recent Asian emission increases on air quality in North America: An integrated analysis using satellite, aircraft, ozonesonde, and surface observations, Atmos. Chem. Phys., 8, 6117-6136, doi:10.5194/acp-8-6117-2008, 2008.

Zhang, L., Li, Q. B., Jin, J., Liu, H., Livesey, N., Jiang, J. H., Mao, Y., Chen, D., Luo, M., and Chen, Y.: Impacts of 2006 Indonesian fires and dynamics on tropical upper tropospheric carbon monoxide and ozone, Atmos. Chem. Phys., 11, 10929–10946, doi:10.5194/acp-11-10929-2011, 2011.

Zhang, Y., Liu, H., Crawford, J. H., Considine, D. B., Chan, C., Oltmans, S. J., and Thouret, V.: Distribution, variability and sources of tropospheric ozone over south China in spring: Intensive ozonesonde measurements at five locations and modeling analysis, J. Geophys. Res., 117, D12304, doi:10.1029/2012JD017498, 2012.

Figure Captions

Figure 1. Locations of Beijing (39.8°N, 116.18°E) and three other ozonesonde stations in north China during the second phase of the TAPTO-China campaign in April-May 2005. Surface topography is shown as color image.

Figure 2. Tropospheric O_3 source regions for tagged O_3 simulations.

Figure 3. GEOS-4 (left panels) and GEOS-5 (right panels) horizontal wind vectors near the surface (lower panels) and ~870hPa (upper panels) in East Asia during April-May 2005. Also shown as a color image are the O_3 concentrations (ppbv) simulated by GEOS-Chem driven with GEOS-4 and GEOS-5 meteorological data sets. Values are averages over April-May. White dots denote the locations of four ozonesonde stations (see Figure 1).

Figure 4. a) Mean vertical profiles of O_3 mixing ratios (ppbv) over Beijing averaged over four days (May 1, May 3, May 11, and May 15) when both ozonesonde (black solid line) and MOZAIC aircraft (red dashed line) measurements were conducted. b) Mean vertical profiles of O_3 mixing ratios observed by ozonesonde and MOZAIC aircraft during April-May 2005 (solid black line), in comparison with GEOS-Chem (blue dashed line) and GMI (orange dotted line) simulations driven by the GEOS-4 meteorological fields. Daily model output was sampled at the time and location of ozonesonde and aircraft measurements. c) Same as b), except that GEOS-Chem and GMI were driven by the GEOS-5 and MERRA meteorological fields, respectively.

Figure 5. Time-height cross-sections of lower-tropospheric O_3 mixing ratios (ppbv), as observed by ozonesonde and MOZAIC aircraft in comparison with GEOS-Chem simulations

driven by the GEOS-4 and GEOS-5 meteorological fields, at Beijing during April-May 2005. Model daily outputs are sampled in the gridbox nearest to Beijing for the dates (vertical lines) of ozonesonde soundings.

Figure 6. Major sources contributing to O_3 (0-6km) over Beijing, as simulated by GEOS-Chem driven by the GEOS-4 meteorological fields during April-May, 2005. The plots show time-height cross-sections of concentrations (ppbv, left panels) and percentages (%, right panels) of tagged O_3 produced in Asian, African, European and North American troposphere, as well as O_3 transported from the stratosphere. Model daily outputs are sampled at the location and dates (vertical lines) of ozonesonde soundings and/or aircraft measurements. Note the different color scales on color bars.

Figure 7. Decreases in the lower-tropospheric O_3 concentrations (ppbv), as simulated by GEOS-Chem driven by the GEOS-4 (left panels) and GEOS-5 (right panels) meteorological fields, when Asian, European, North American fossil fuel emissions, biomass burning emissions, or lightning NO_x emissions were suppressed, respectively, relative to their standard simulations for April-May, 2005. Note the different scales on color bars. Colors are saturated when values are out of range.

Figure 8. Timeseries of O_3 concentrations (ppbv, red line) and temperature (balck line) at 878 hPa over Beijing in the GEOS-Chem model driven by the GEOS-4 meteorological fields. Also shown in the panel are simulated concentrations (ppbv) of tagged O_3 produced in the Asian (AS, grey line), African (AF, purple line), European (EU, orange line), and North American (NA, blue line) troposphere, and O_3 transported from the stratosphere (Strat, green line). Vertical lines indicate dates with ozonesonde soundings and/or aircraft measurements.

Figure 9. Vertical profiles of O_3 mixing ratios (ppbv) over Beijing from ozonesonde (black solid line) and MOZAIC aircraft (blue solid line) measurements on May 3, 2005, in comparison with those simulated by GEOS-Chem/GEOS-4 (green dashed line) and GMI/GEOS-4 (blue dotted line). Sonde-observed RH (%) and temperature (°C) are shown as red solid line and purple solid line, respectively. Decreases in O_3 concentrations (ppbv) when Asian fossil fuel or lightning NO_x emissions were suppressed, relative to the standard simulation, are shown as orange and purple dot-dashed lines, respectively. O_3 transported down from the stratosphere (ppbv) is shown as pink dot-dashed line.

Figure 10. Five-day back trajectories arriving at the altitudes of 150m (green line), 1400m (blue line), and 2400m (red line), respectively, over Beijing at 1400LT on May 3, 2005. AGL denotes the altitudes above ground level. The ozonesonde station is 34m asl.

Figure 11. Average CO concentrations (ppbv, left panels) and O_3 concentrations (ppbv, right panels) in the lower troposphere (797hPa, top panels; 878hPa, middle panels; 942 bottom panels) over East Asia on May 2, 2005, as simulated by GEOS-Chem driven by the GEOS-4 meteorological fields. Dots denote the locations of four ozonesonde stations shown in Figure 1. Arrows are wind vectors. Note the different arrow scales for wind vectors at different levels.

Figure 12. Same as Figure 11, but for May 3, 2005.

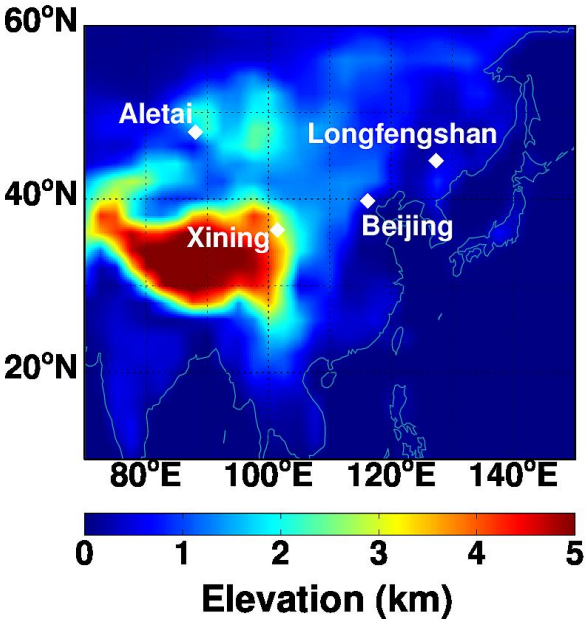

Figure 1. Locations of Beijing (39.8°N, 116.18°E) and three other ozonesonde stations in north China during the second phase of the TAPTO-China campaign in April-May 2005. Surface topography is shown as color image.

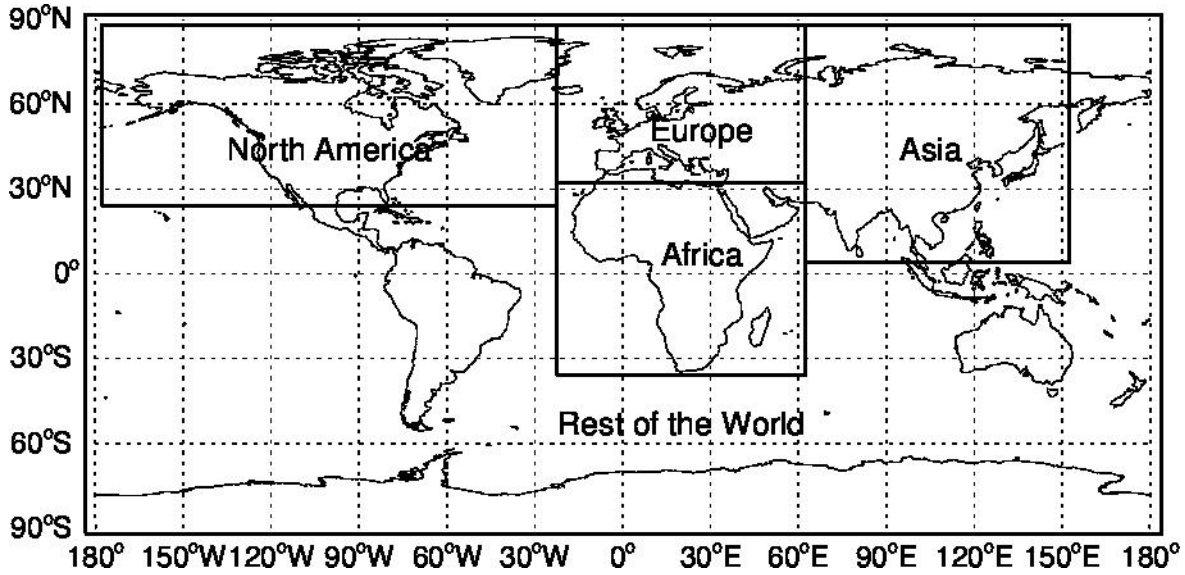

Figure 2. Tropospheric O_3 source regions for tagged O_3 simulations.

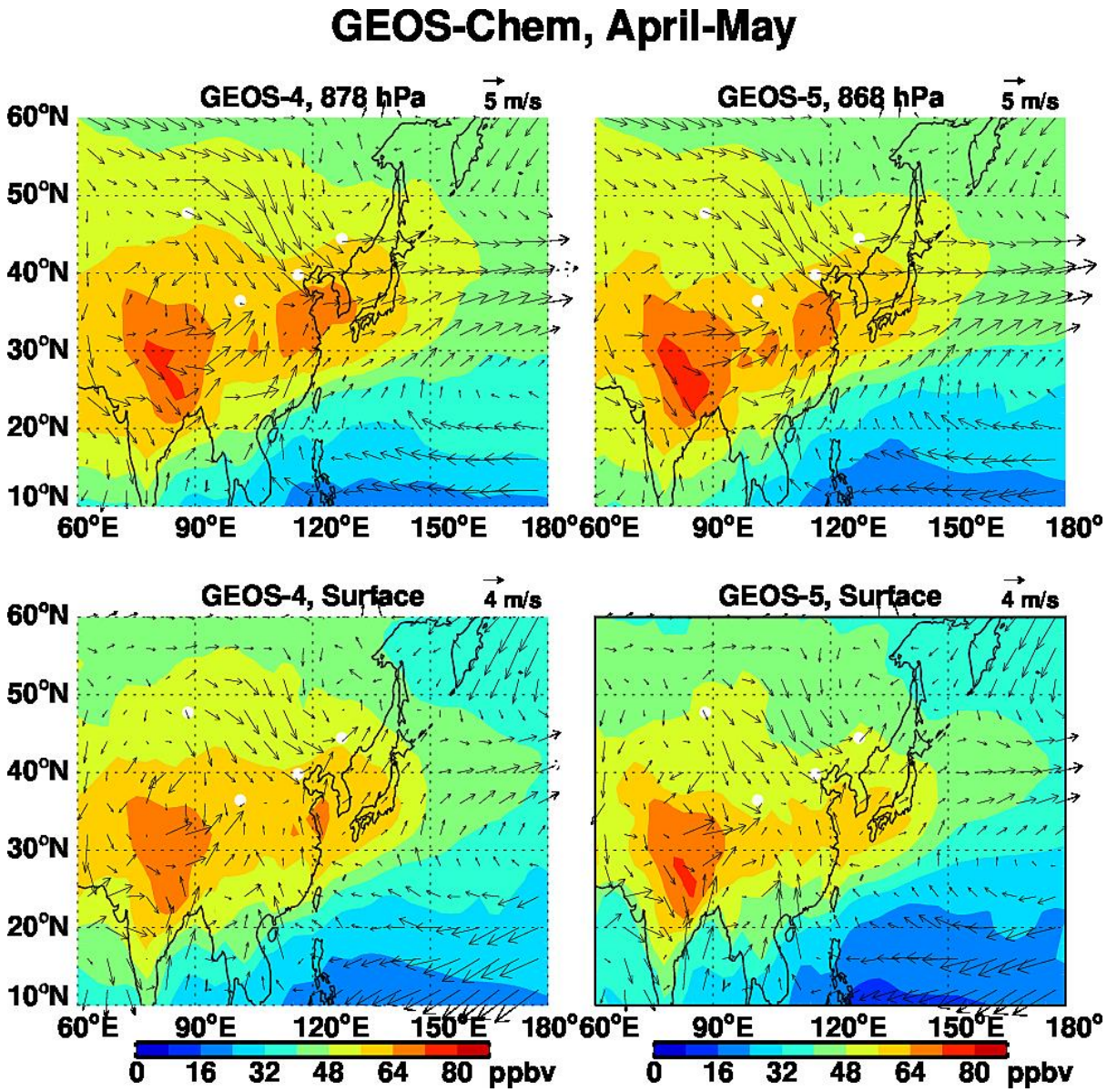

Figure 3. GEOS-4 (left panels) and GEOS-5 (right panels) horizontal wind vectors near the surface (lower panels) and ~870hPa (upper panels) in East Asia during April-May 2005. Also shown as a color image are the O_3 concentrations (ppbv) simulated by GEOS-Chem driven with GEOS-4 and GEOS-5 meteorological data sets. Values are averages over April-May. White dots denote the locations of four ozonesonde stations (see Figure 1).

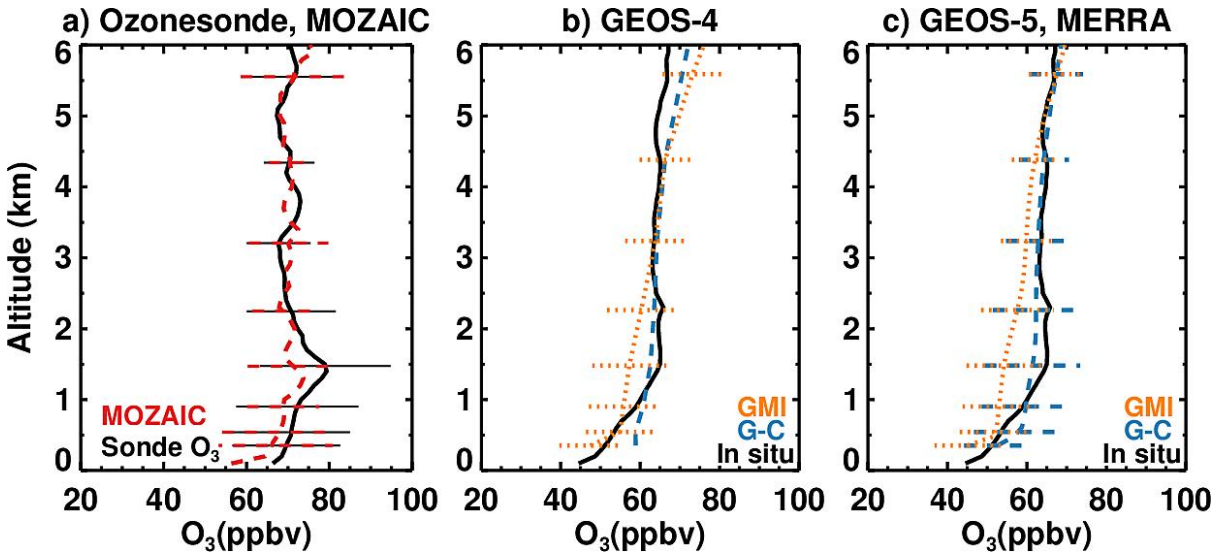

Figure 4. a) Mean vertical profiles of O_3 mixing ratios (ppbv) over Beijing averaged over four days (May 1, May 3, May 11, and May 15) when both ozonesonde (black solid line) and MOZAIC aircraft (red dashed line) measurements were conducted. b) Mean vertical profiles of O_3 mixing ratios observed by ozonesonde and MOZAIC aircraft during April-May 2005 (solid black line), in comparison with GEOS-Chem (blue dashed line) and GMI (orange dotted line) simulations driven by the GEOS-4 meteorological fields. Daily model output was sampled at the time and location of ozonesonde and aircraft measurements. c) Same as b), except that GEOS-Chem and GMI were driven by the GEOS-5 and MERRA meteorological fields, respectively.

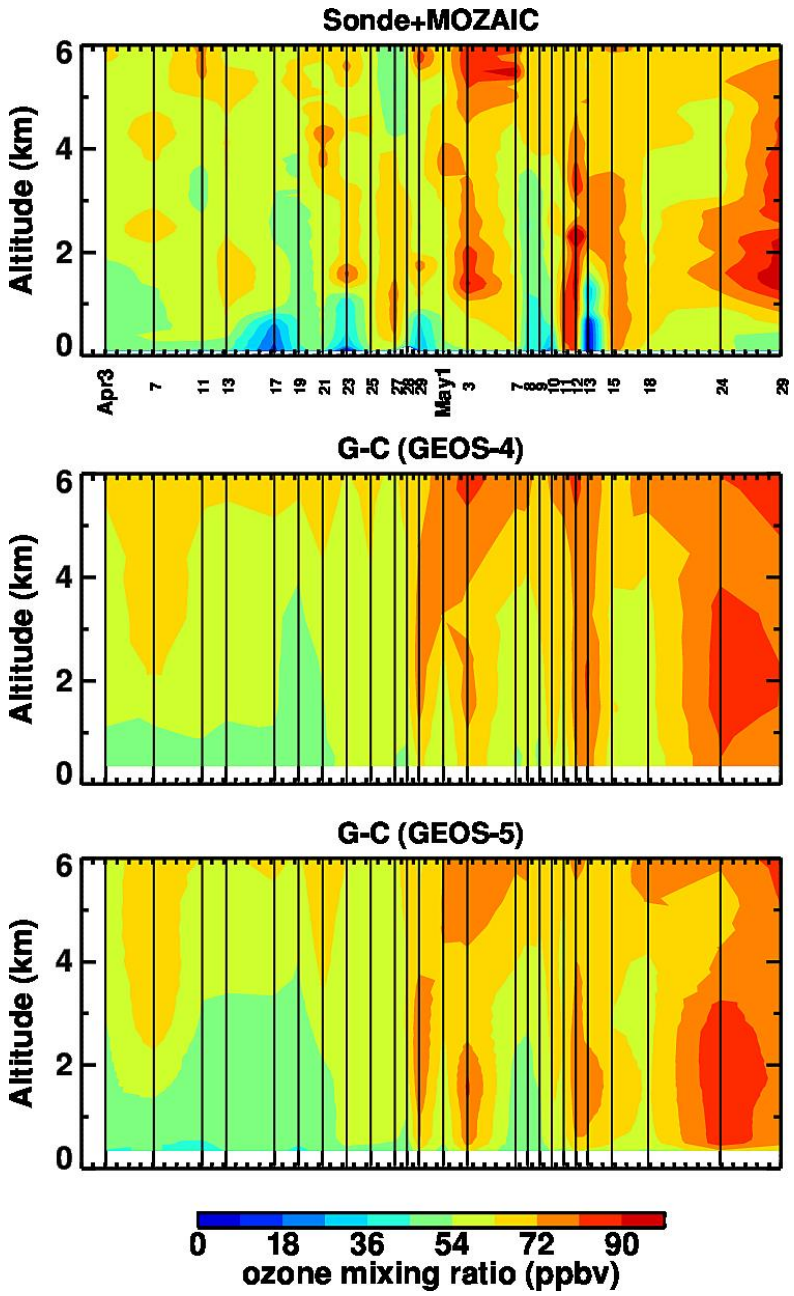

Figure 5. Time-height cross-sections of lower-tropospheric O_3 mixing ratios (ppbv), as observed by ozonesonde and MOZAIC aircraft in comparison with GEOS-Chem simulations driven by the GEOS-4 and GEOS-5 meteorological fields, at Beijing during April-May 2005. Model daily outputs are sampled in the gridbox nearest to Beijing for the dates (vertical lines) of ozonesonde soundings.

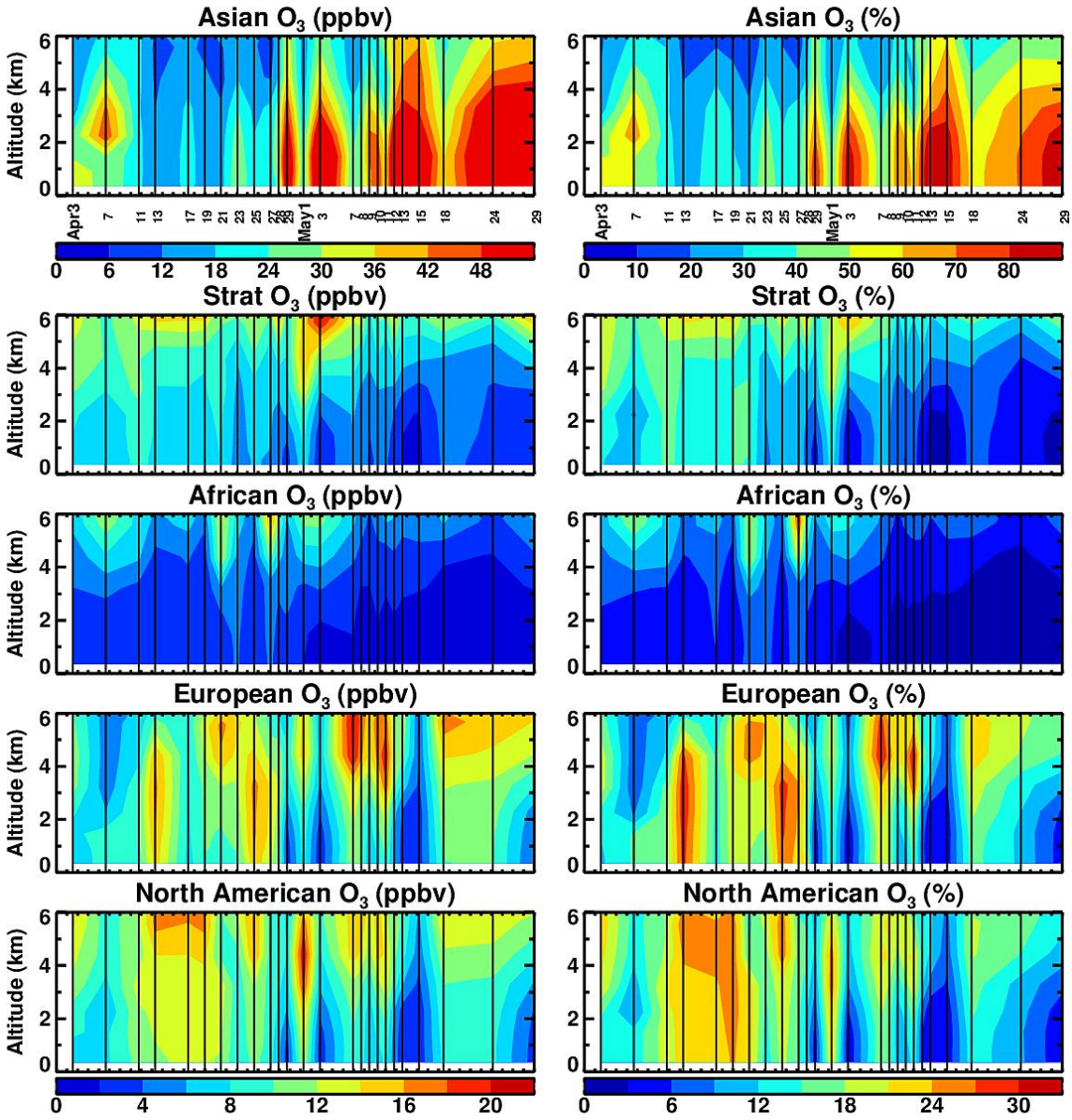

Figure 6. Major sources contributing to O_3 (0-6km) over Beijing, as simulated by GEOS-Chem driven by the GEOS-4 meteorological fields during April-May, 2005. The plots show time-height cross-sections of concentrations (ppbv, left panels) and percentages (%, right panels) of tagged O_3 produced in Asian, African, European and North American troposphere, as well as O_3 transported from the stratosphere. Model daily outputs are sampled at the location and dates (vertical lines) of ozonesonde soundings and/or aircraft measurements. Note the different color scales on color bars.

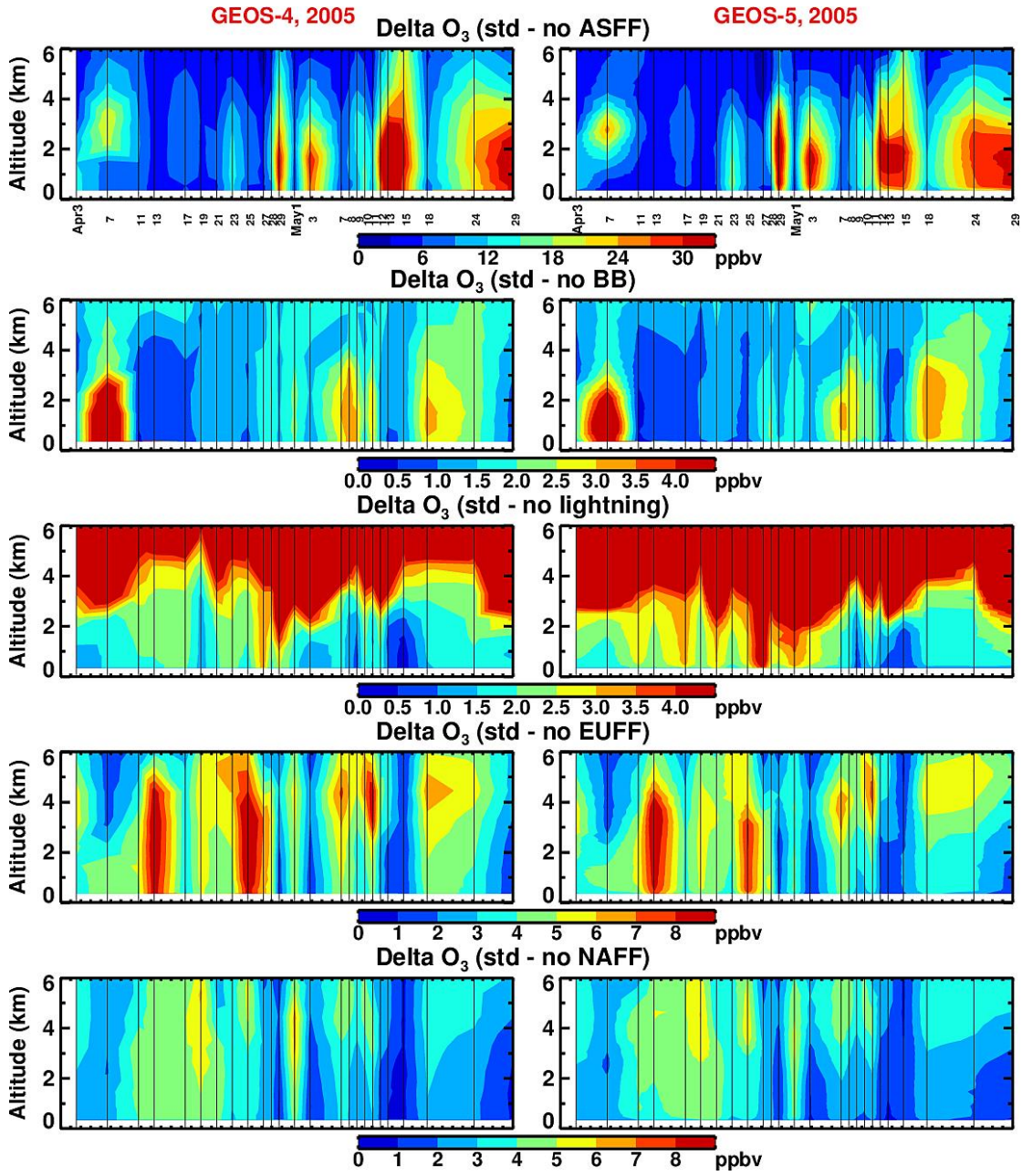

Figure 7. Decreases in the lower-tropospheric O_3 concentrations (ppbv), as simulated by GEOS-Chem driven by the GEOS-4 (left panels) and GEOS-5 (right panels) meteorological fields, when Asian, European, North American fossil fuel emissions, biomass burning emissions, or lightning NO_x emissions were suppressed, respectively, relative to their standard simulations for April-May, 2005. Note the different scales on color bars. Colors are saturated when values are out of range.

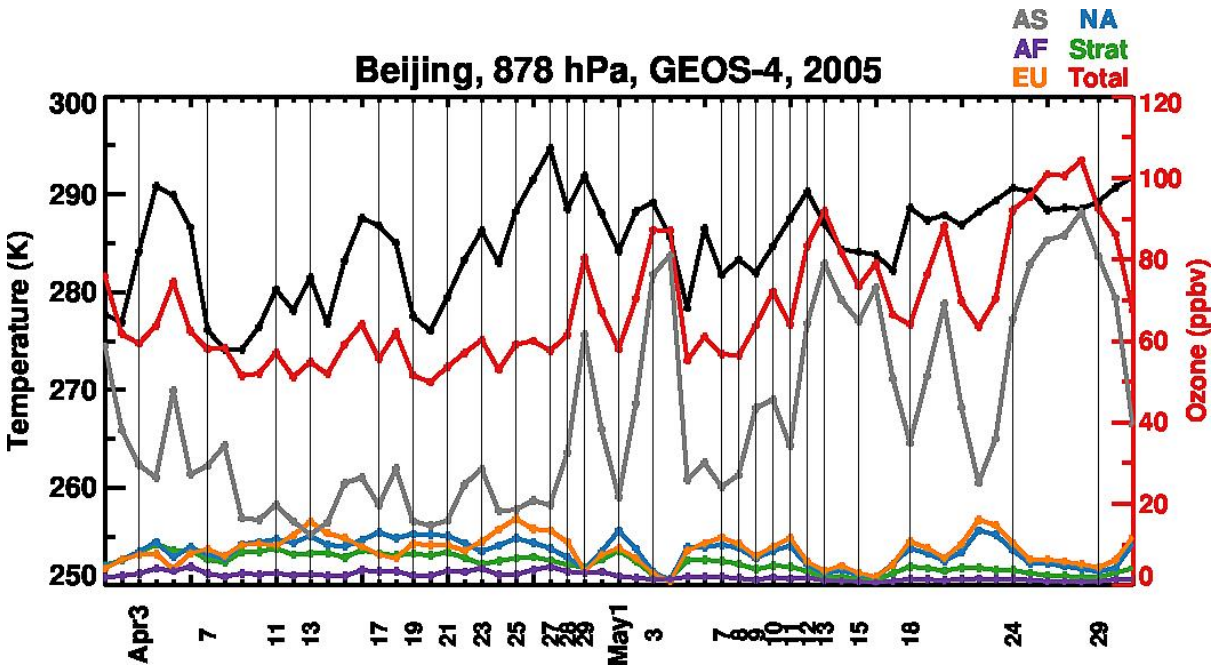

Figure 8. Timeseries of O_3 concentrations (ppbv, red line) and temperature (balck line) at 878 hPa over Beijing in the GEOS-Chem model driven by the GEOS-4 meteorological fields. Also shown in the panel are simulated concentrations (ppbv) of tagged O_3 produced in the Asian (AS, grey line), African (AF, purple line), European (EU, orange line), and North American (NA, blue line) troposphere, and O_3 transported from the stratosphere (Strat, green line). Vertical lines indicate dates with ozonesonde soundings and/or aircraft measurements.

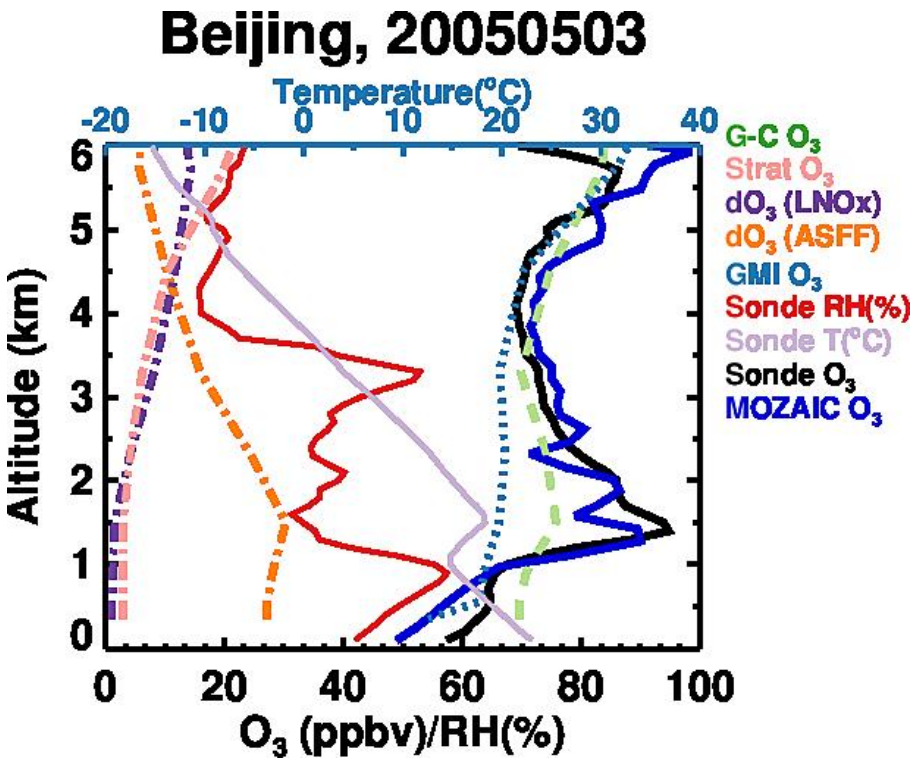

Figure 9. Vertical profiles of O_3 mixing ratios (ppbv) over Beijing from ozonesonde (black solid line) and MOZAIC aircraft (blue solid line) measurements on May 3, 2005, in comparison with those simulated by GEOS-Chem/GEOS-4 (green dashed line) and GMI/GEOS-4 (blue dotted line). Sonde-observed RH (%) and temperature (°C) are shown as red solid line and purple solid line, respectively. Decreases in O_3 concentrations (ppbv) when Asian fossil fuel or lightning NO_x emissions were suppressed, relative to the standard simulation, are shown as orange and purple dot-dashed lines, respectively. O_3 transported down from the stratosphere (ppbv) is shown as pink dot-dashed line.

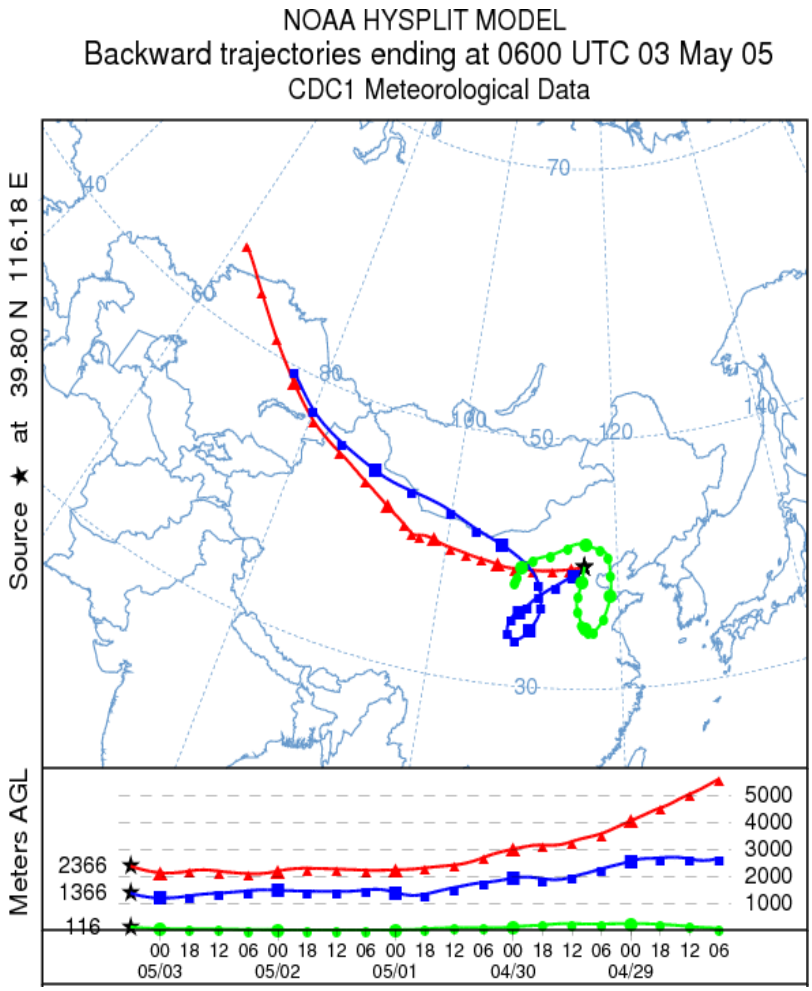

Figure 10. Five-day back trajectories arriving at the altitudes of 150m (green line), 1400m (blue line), and 2400m (red line), respectively, over Beijing at 1400LT on May 3, 2005. AGL denotes the altitudes above ground level. The ozonesonde station is 34m asl.

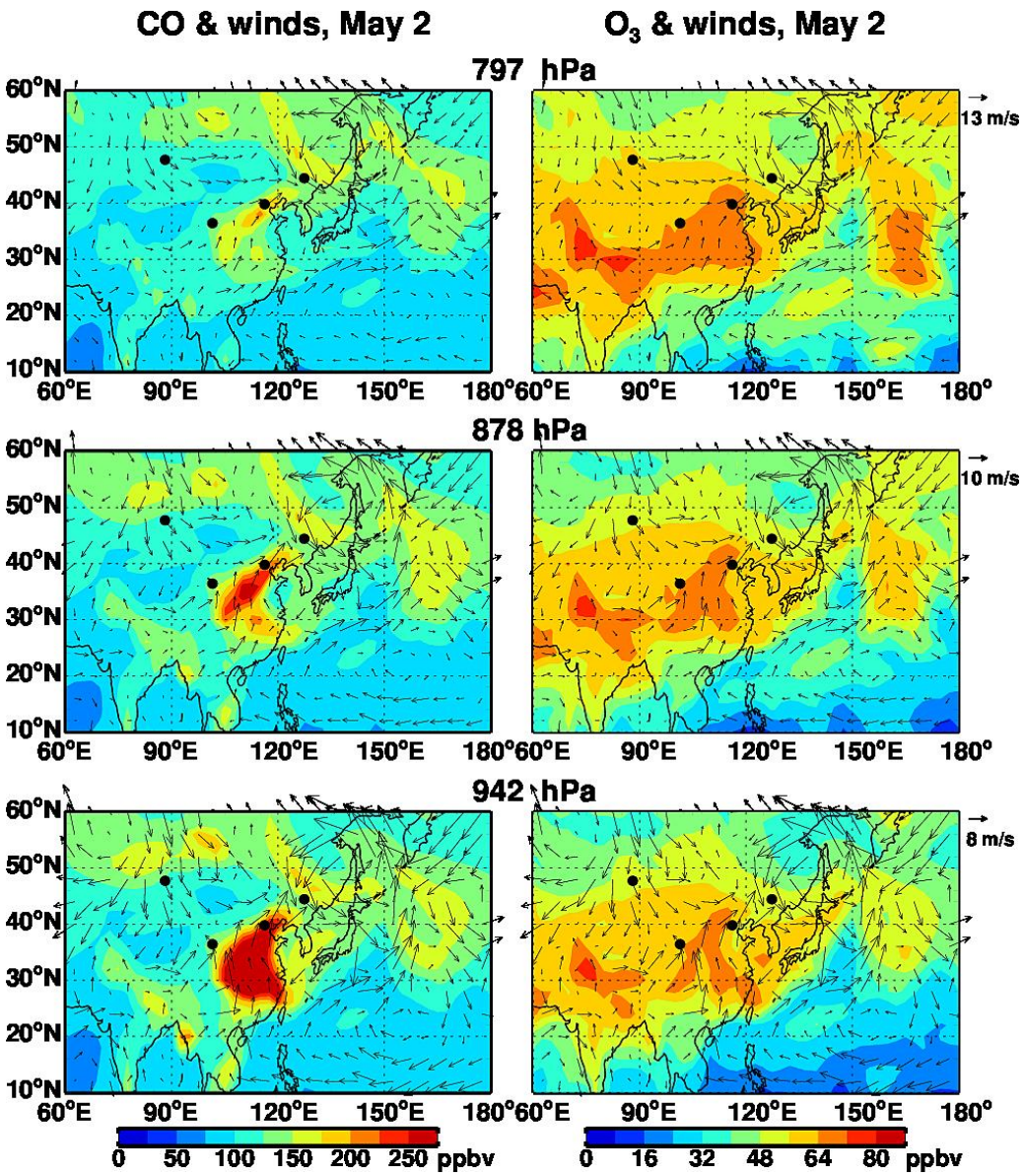

Figure 11. Average CO concentrations (ppbv, left panels) and O_3 concentrations (ppbv, right panels) in the lower troposphere (797hPa, top panels; 878hPa, middle panels; 942 bottom panels) over East Asia on May 2, 2005, as simulated by GEOS-Chem driven by the GEOS-4 meteorological fields. Dots denote the locations of four ozonesonde stations shown in Figure 1. Arrows are wind vectors. Note the different arrow scales for wind vectors at different levels.

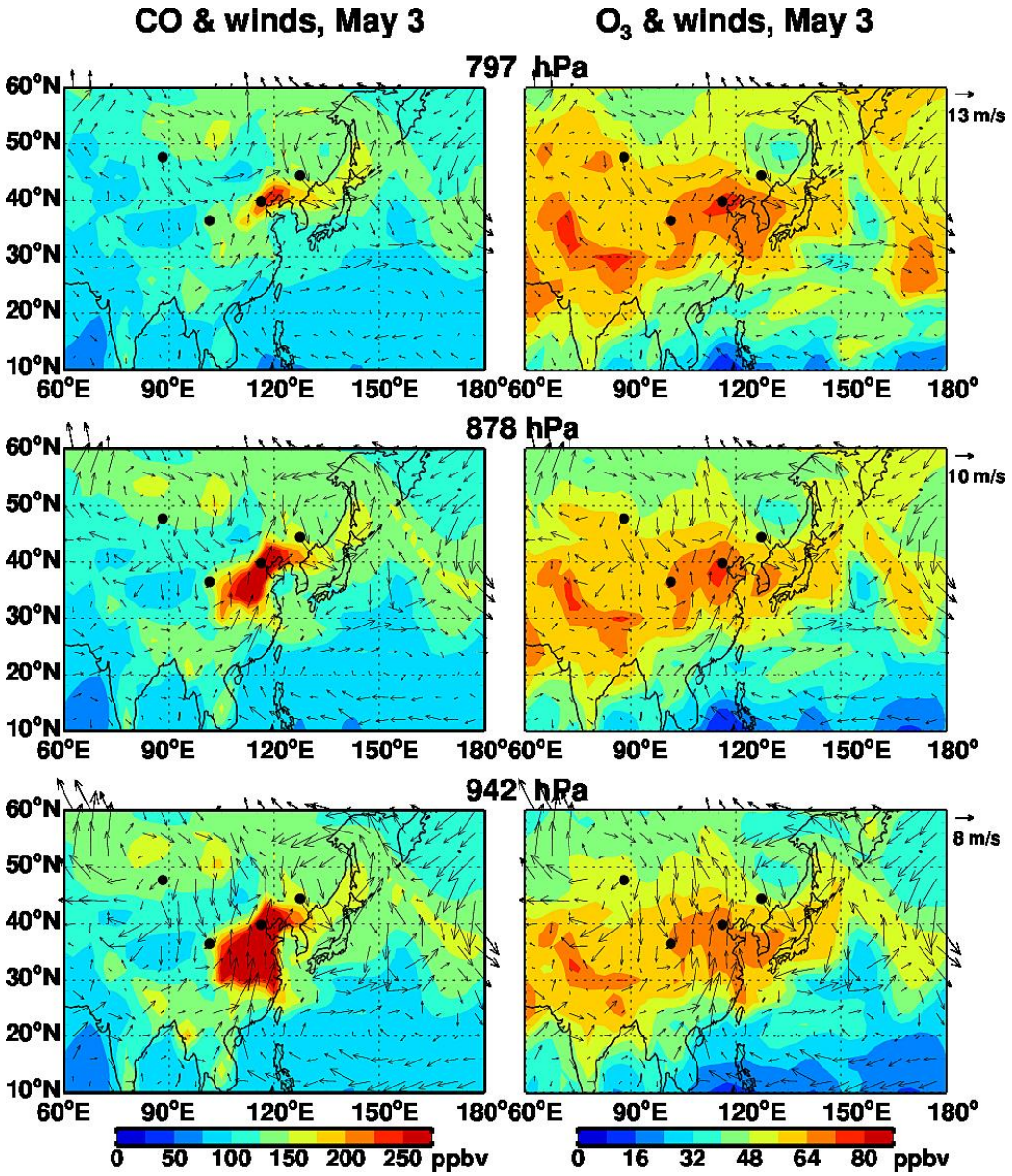

Figure 12. Same as Figure 11, but for May 3, 2005.